SIMDET 2025

Uses of SYNOPSYS TCAD in High-Energy Physics Experiments

Modeling, Simulation, and Applications

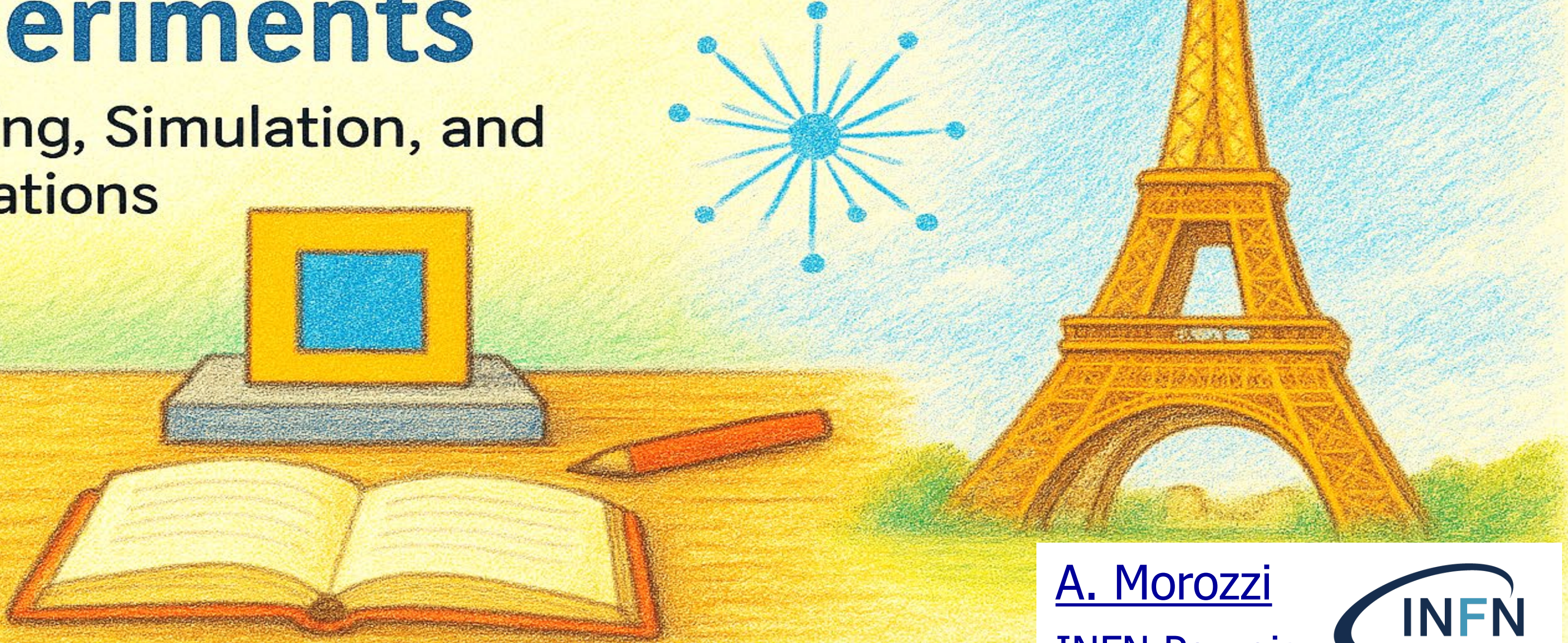

A. Morozzi
INFN Perugia
INFN Istituto Nazionale di Fisica Nucleare

Outline

- Motivation & Challenges
- Device-level & Mixed mode simulations
  - Radiation damage effects models
  - Next generation silicon detectors
  - Rad-Hard and innovative materials
- Combine TCAD and AllPix Squared
- Conclusions

Selective, non-complete set of examples from HEP experiments

arianna.morozzi@pg.infn.it

Motivations and Challenges

- **Performance of complex sensors is not analytically predictable anymore!**
  → Increasing need for TCAD simulations.
- Semiconductor detectors will face increasing radiation levels
  - >1×10^{16} 1MeV n_{eq}/cm^2 (HL-LHC);
  - >5×10^{17} 1MeV n_{eq}/cm^2 (FCC-hh);
    - detectors used at LHC cannot be operated after such irradiation.
- New requirements lead to new detector technologies
  - Need to be optimized for radiation hardness and/or 4D tracking capabilities.
- Modern TCAD simulation tools can have a crucial role in radiation-hard device design
  - Reducing costly and time-consuming physical testing.
  - To get insights. Deep understanding of physical device behavior.
  - To quickly screen technological options and drive the industrial strategy.
  - Combined Bulk and surface radiation damage can be considered.
  - Within a hierarchical approach, increasingly complex models can be considered, by balancing complexity and comprehensiveness.

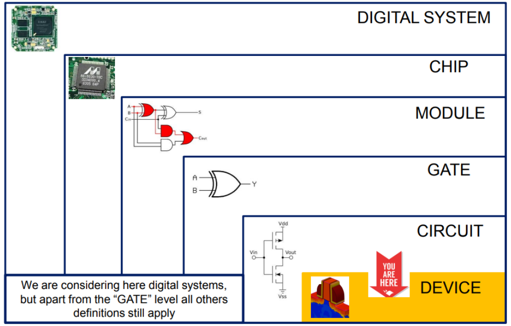

arianna.morozzi@pg.infn.it

The Technology-CAD modeling approach

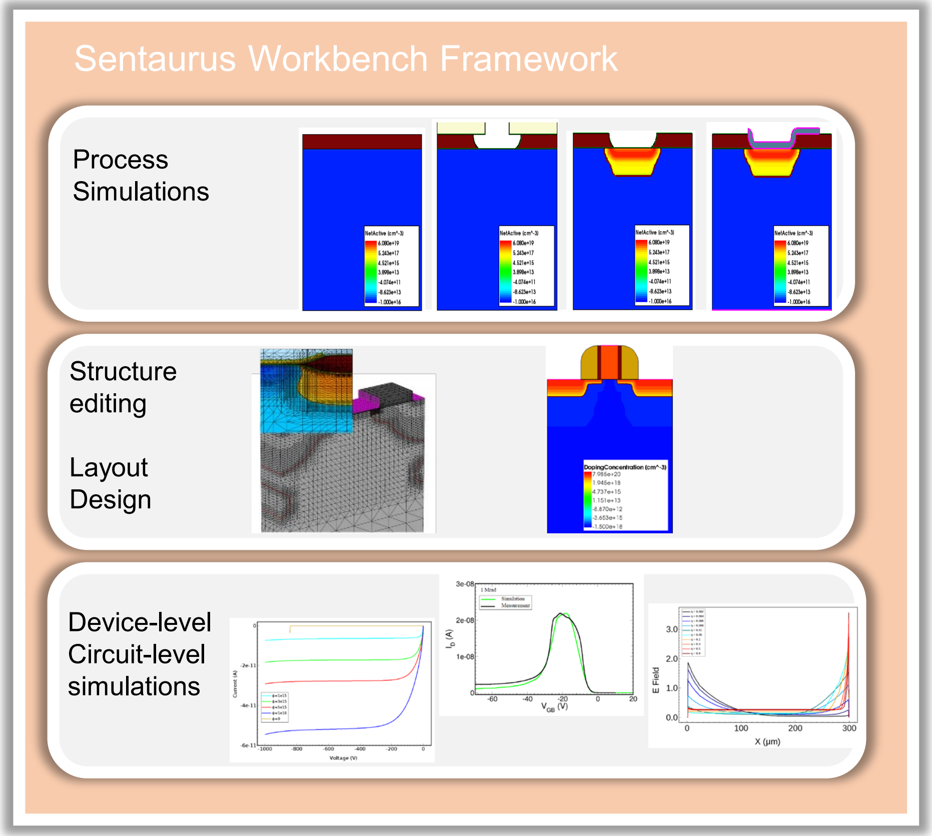

- √ TCAD simulation tools solve fundamental, physical partial differential equations, such as diffusion and transport equations for discretized geometries (finite element meshing).
- √ This deep physical approach gives TCAD simulation predictive accuracy.
- ✓ Synopsys© Sentaurus TCAD

$$\begin{cases} \nabla\cdot\left(-\varepsilon_s\nabla\varphi\right)=q\left(N_D^{+}-N_A^{-}+p-n\right) & \text{Poisson} \\ \dfrac{\partial n}{\partial t}-\dfrac{1}{q}\nabla\cdot\vec{J}_n=G-R & \text{Electron continuity} \\ \dfrac{\partial p}{\partial t}+\dfrac{1}{q}\nabla\cdot\vec{J}_p=G-R & \text{Hole continuity} \end{cases}$$

$$\vec{J}_n=-q\mu_n n\nabla\varphi+qD_n\nabla n$$

$$\vec{J}_p=-q\mu_p p\nabla\varphi-qD_p\nabla p$$

Radiation damage models

Synopsys Sentaurus TCAD Sdevice simulations
for HEP experiments

arianna.morozzi@pg.infn.it

TCAD models - an overview

Different approaches to TCAD radiation damage modeling:

- ✓ EVL Model (2 levels)
- ✓ Delhi-2014 (2 levels)
- ✓ KIT (Eber) (2 levels)
- ✓ New Univ. Of Perugia Bulk+Surface (3 levels)
- ✓ Folkestad (CERN model)/LHCb (3 levels)
- ✓ Hamburg Penta Trap Model (HPTM) (5 levels)

Different modeling approaches (traps, energy levels and related parameters), often tailored to specific datasets and devices.

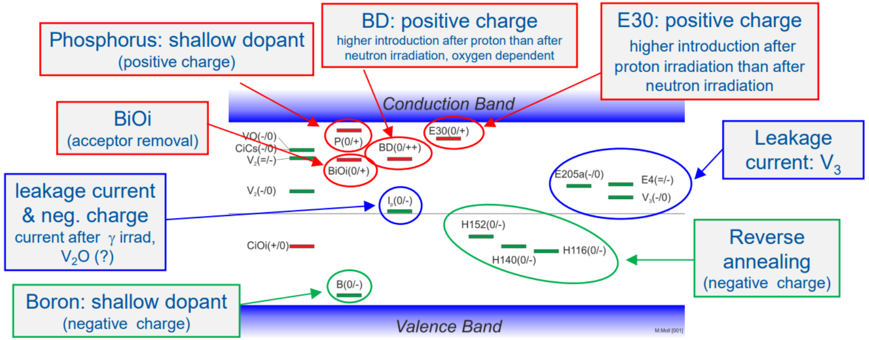

RD50 map of most relevant defects for device performance near RT

GOAL: General purpose TCAD model (DRD3 WP4 - ECFA Detector R&D Roadmap)

- Not over specific
  → set of "effective" defects within the semiconductor bandgap.
- Predictive capabilities to be extended $\Phi > 10^{16}$ n_{eq}/cm^2.
- Accounts for different irradiation levels and particle types.

Hamburg Penta Trap Model (HPTM)

- HPTM with 5 effective traps
  - Developed to simulate the I-V, C-V and CCE with IR of diodes for various fluence levels and use the TCAD optimizer to determine the free parameters i.e., minimize simultaneously for every fluence.
- Optimize the performance of pad diodes irradiated with 24 GeV/c p in the fluence range of $3{\cdot}10^{14}$ to $1.3{\cdot}10^{16}$ n_{eq}/cm^{-2}.
- Charge trapping is essential to predict the response of radiation-damaged segmented sensors, due to the highly non-uniform weighting field.

Result of tuning: Hamburg Penta Trap Model (HPTM)

Defect	Type	Energy	g_{int} [cm^{-1}]	σ_e [cm^2]	σ_h [cm^2]
E30K	Donor	E_C-0.1 eV	0.0497	2.300E-14	2.920E-16
V_3	Acceptor	E_C-0.458 eV	0.6447	2.551E-14	1.511E-13
I_p	Acceptor	E_C-0.545 eV	0.4335	4.478E-15	6.709E-15
H220	Donor	E_V+0.48 eV	0.5978	4.166E-15	1.965E-16
C_iO_i	Donor	E_V+0.36 eV	0.3780	3.230E-17	2.036E-14

- Trap concentration of defects: $\mathbf{N = g_{int} \cdot \Phi_{neq}}$
- Simulations for the optimization have been performed at **T= -20 °C** with:
  1. Slotboom band gap narrowing
  2. Impact ionisation (van Overstaeten-de Man)
  3. Trap Assisted Tunneling Hurkx with tunnel mass = **0.25 m_e** (default value: 0.5 m_e) in case of the I_p
  4. Relative permittivity of silicon = 11.9 (default value: 11.7)
- Both cross section for the E30K and the electron cross section for the C_iO_i were fixed ➔ 12 free parameter
- Optimization done with the nonlinear simplex method

Comparison with strips

Simulated structure

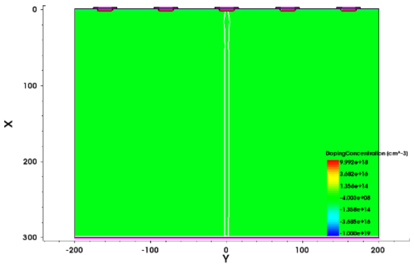

Collected charge vs. fluence

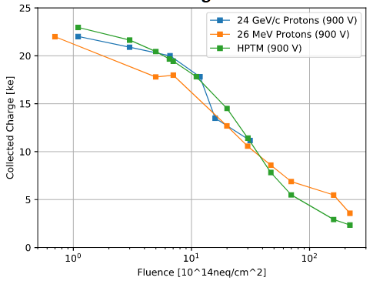

- Float zone silicon
- 300 um thick sensors
- 80 um pitch
- T = -25 °C
- ^{90}Sr source

Data from A. Affolder et al., NIMA Vol. 623 (2010), pp. 177-179.

J. Schwandt, arXiv:1904.10234.
J. Schwandt, IEEE NSS MIC 2028 talk.

INFN arianna.morozzi@pg.infn.it

HPTM Simulation results

I-V for fluences from 0.3 - 13•10^{15} n_{eq}/cm² at T= -20 °C (for T= -30 °C see backup)

I-V

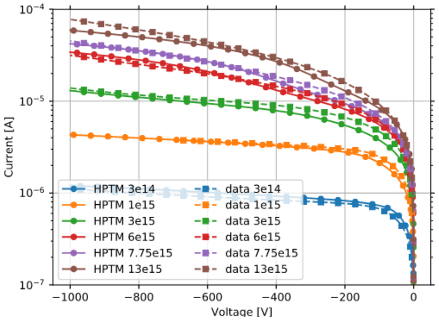

ratio simulation / data

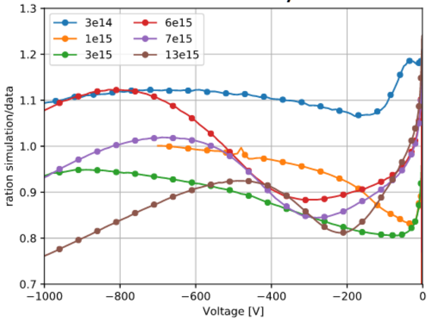

C-V for fluences from 0.3 - 13•10^{15} n_{eq}/cm² at 455 Hz and T = -20 °C (for T= -30 °C see backup)

1/C²-V

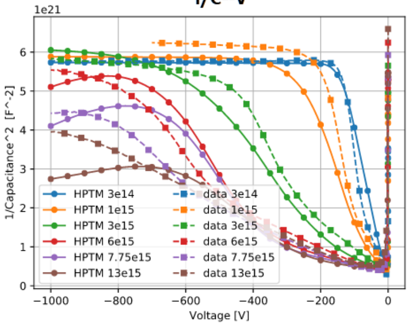

ratio simulation / data

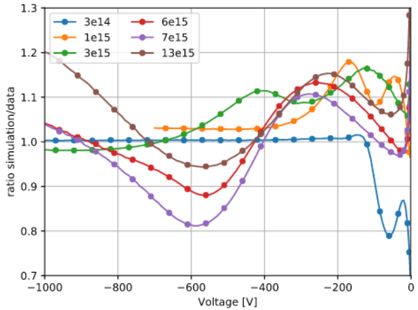

CCE vs. V for fluences from 0.3 - 13•10^{15} n_{eq}/cm² with infrared laser and T = -20 °C (for T= -30 °C see backup)

CCE-V

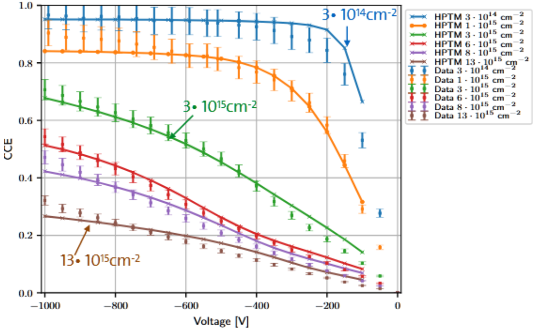

ratio simulation / data

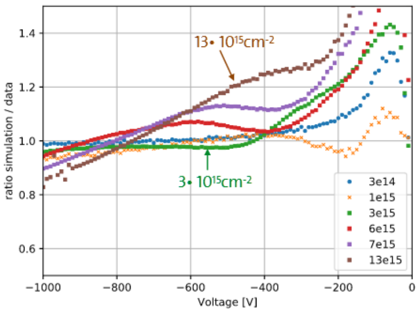

T= -20°C, 60min at 80°C

J. Schwandt, arXiv:1904.10234.
J. Schwandt, IEEE NSS MIC 2028 talk.

CERN bulk radiation damage model (Folkestad)

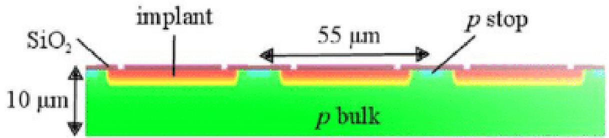

From the classical **EVL model***, one donor and one acceptor level (1 and 2 in the table), they add a third acceptor level. Cross-sections are adjusted to experimental results. Measurements for 200 µm thick n-on-p sensors bump bonded to TimePix3 readout .

Simulated electric field (2D mesh) in pixel centre at 1000V bias for two fluence levels.

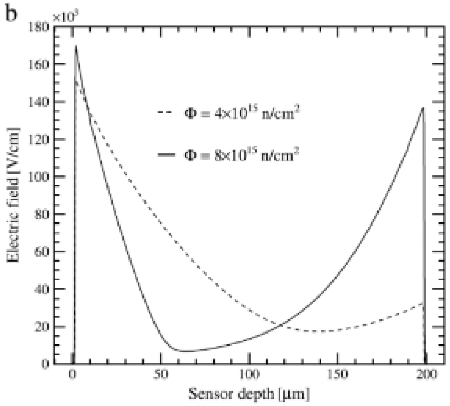

Parameters of the proposed radiation damage model. The energy levels are given with respect to the valence band (E_V) or the conduction band (E_C). The model is intended to be used in conjunction with the Van Overstraeten–De Man avalanche model.

Defect number	Type	Energy level [eV]	σ_e [cm^{-2}]	σ_h [cm^{-2}]	η [cm^{-1}]
1	Donor	$E_V + 0.48$	2×10^{-14}	1×10^{-14}	4
2	Acceptor	$E_C - 0.525$	5×10^{-15}	1×10^{-14}	0.75
3	Acceptor	$E_V + 0.90$	1×10^{-16}	1×10^{-16}	36

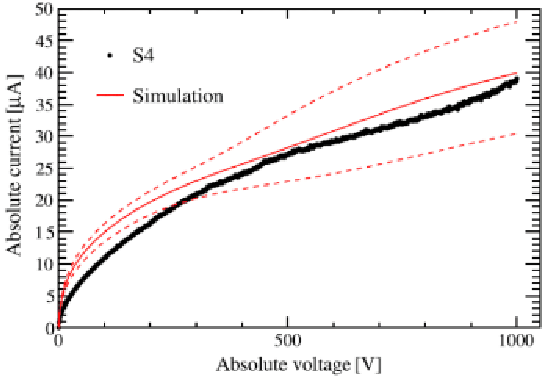

Measured and simulated I-V curves (T=-31,1ºC) after uniform proton irradiation to Φ=4e15 MeV n_{eq}/cm^2.

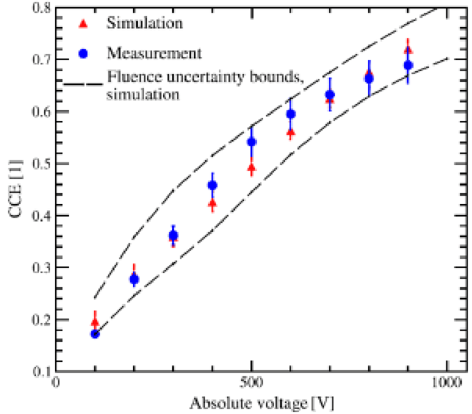

Measured and simulated CCE as a function of voltage at Φ=4e15 MeV n_{eq}/cm^2.

The model captures the transition from a linear electric field/saturating I-V curve to a double junction electric field/non-saturating I-V curve, as a consequence of avalanche generation in the high-field regions of doublé junctions. For pixel center hit, the CCE is aceptable.

A. Folkestad et al., NIM A 874 (2017) pp. 94-102
F.R. Palomo, VERTEX2019

3Ds

Columnar vs Trench

From planar to 3D

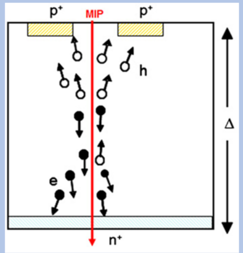

Schematic cross-sections planar sensors

ADVANTAGES:
- Easy to fabricate;
- Low capacitance.

DISADVANTAGES:
- High full depletion voltage;
- Low temporal resolution.

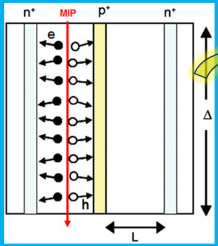

Schematic cross-sections 3D sensors

ADVANTAGES:
- Low depletion voltage;
- High Radiation tolerance.

DISADVANTAGES:
- High capacitance;
- Complicated fabrication technology.

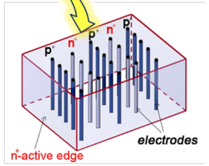

First generation design

Features:
High radiation tolerance;
High fabrication yield.

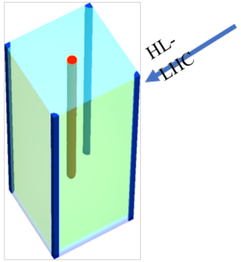

Small pitch 3D pixel sensors

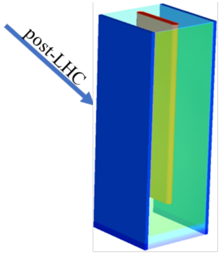

3D trench-electrode sensors

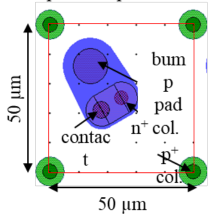

Layout of Small pitch 3D pixel sensors

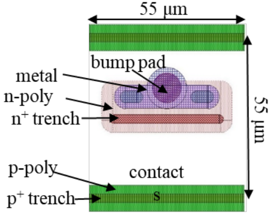

Layout of 3D trench-electrode sensors

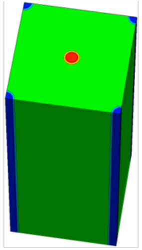

50×50-1E Simulation Domain

2D cut

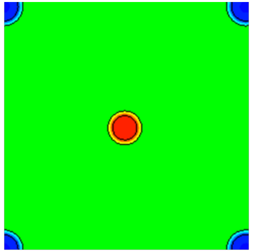

2D cut

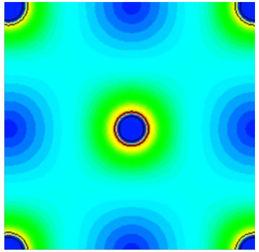

Electric Field, V_b=100V

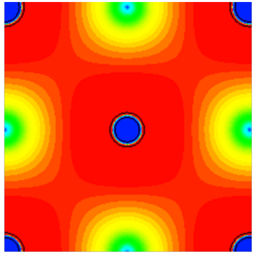

Electron Drift Velocity V_b=100V

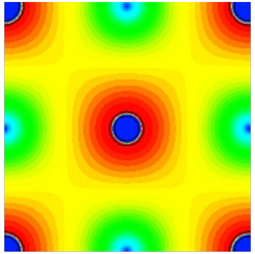

Hole Drift Velocity V_b=100V

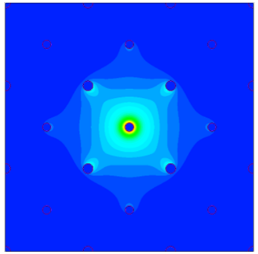

Weighting Field of 3×3 array

Small pitch 3D pixel sensors - - 2D Domain

Material courtesy of G.-F. Dalla Betta

Small pitch 3D pixel sensors – 3D Domain

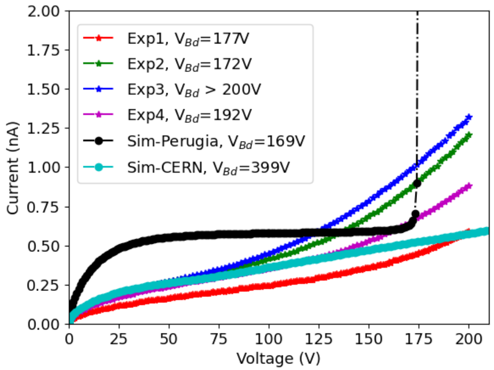

Fluence = 1E16 n_{eq}/cm^2

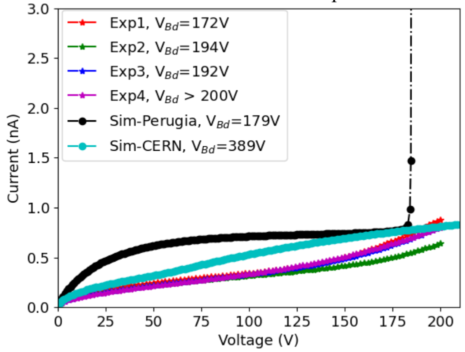

Fluence = 2E16 n_{eq}/cm^2

CERN bulk damage model reproduces better leakage current

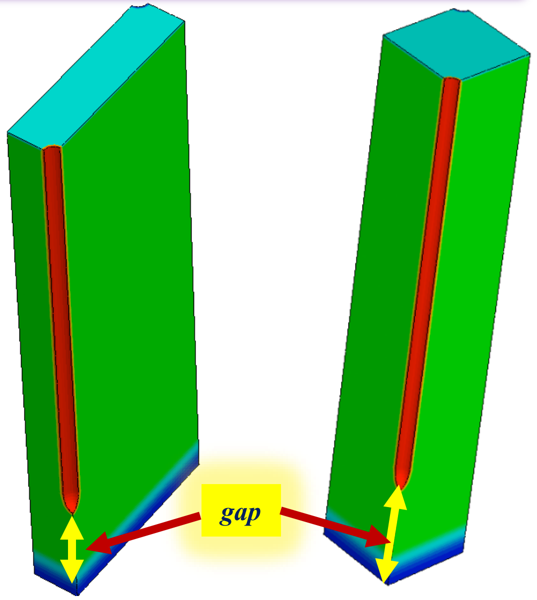

Simulation domain 25×100-1E

Simulation domain 50×50-1E

Perugia bulk damage model is better at predicting the breakdown voltage

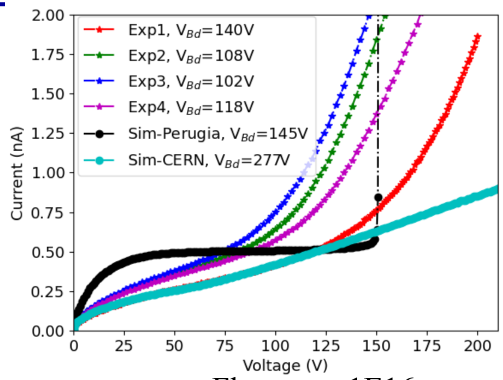

Fluence = 1E16

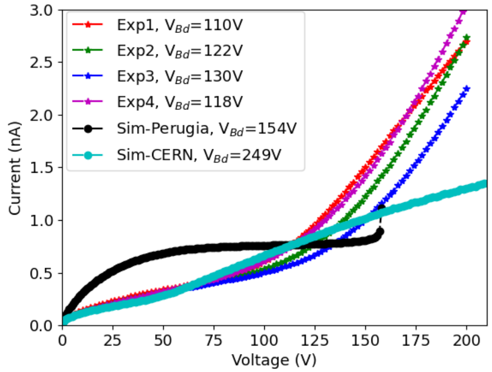

Fluence = 2E16

Material courtesy of G.-F. Dalla Betta

The "New Univ. of Perugia" model - at a glance

√ Surface damage (+ Q_{OX})

Type	Energy (eV)	Band width (eV)	Conc. (cm^{-2})
Acceptor	$E_C \le E_T \le E_C$-0.56	0.56	$D_{IT} = D_{IT}(\Phi)$
Donor	$E_V \le E_T \le E_V$+0.6	0.60	$D_{IT} = D_{IT}(\Phi)$

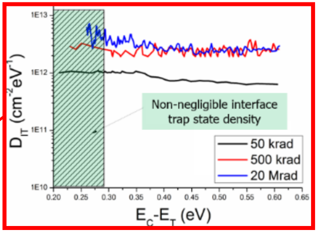

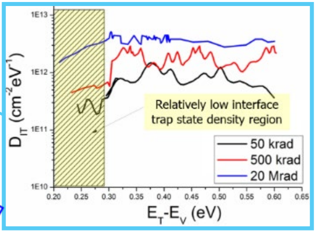

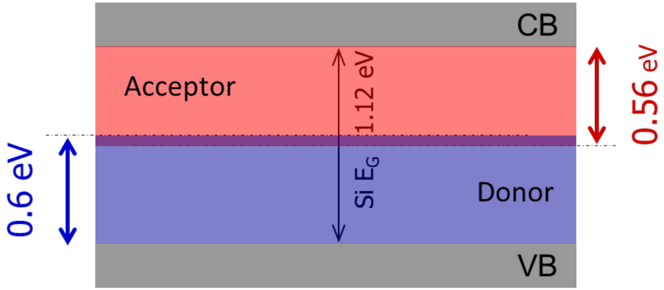

√ Bulk damage

Avalanche ON: Van Overstraeten–De Man (default)

Type	Energy (eV)	η (cm^{-1})	σ_n (cm^2)	σ_h (cm^2)
Donor	E_C - 0.23	0.006	2.3×10^{-14}	2.3×10^{-15}
Acceptor	E_C - 0.42	1.6	1×10^{-15}	1×10^{-14}
Acceptor	E_C - 0.46	0.9	7×10^{-14}	7×10^{-13}

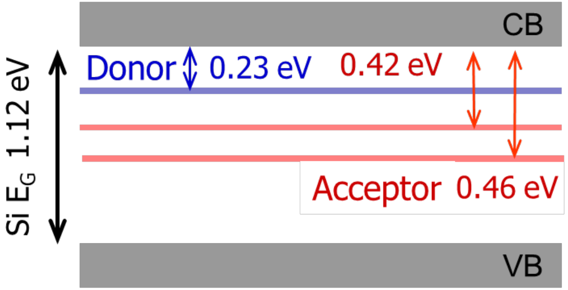

A. Morozzi et al., Front. Phys., 9 (2021)

arianna.morozzi@pg.infn.it

The "New Univ. of Perugia" model – flow

The overall modelling approach pursued

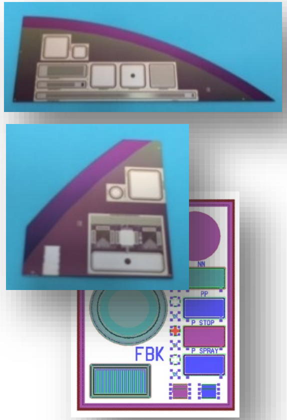

TEST STRUCTURE MEASUREMENTS

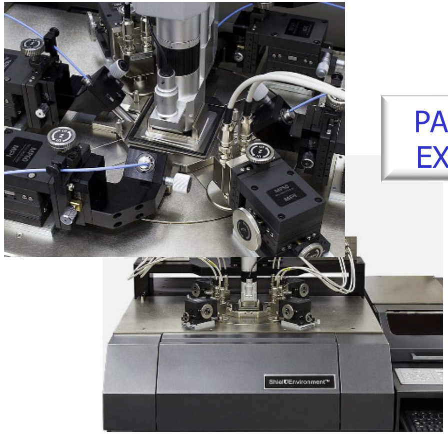

PARAMETERS EXTRACTION

MODEL

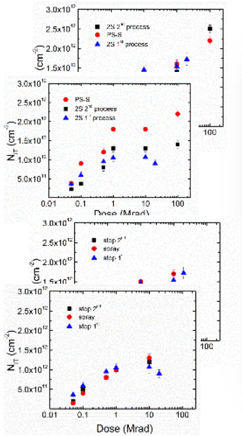

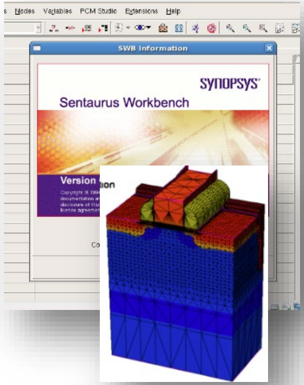

MODEL VALIDATION

DETECTOR OPTIMIZATION

CCE, I-V, C-V, …

- √ Modeling the effects of the radiation damage.
- √ Predictive insight into the behavior of detectors, aiming at their performance optimization.

arianna.morozzi@pg.infn.it

Surface model validation: MOS capacitors

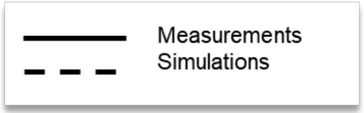

IFX MOS Capacitors

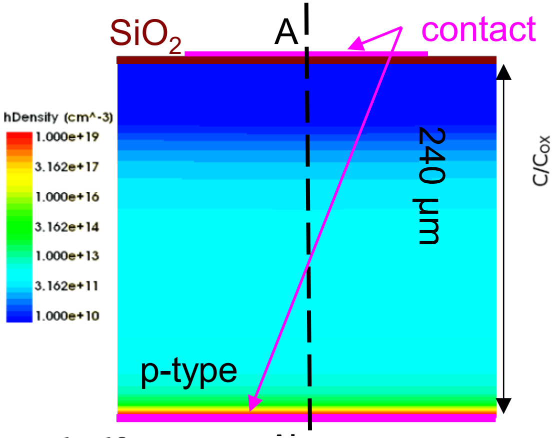

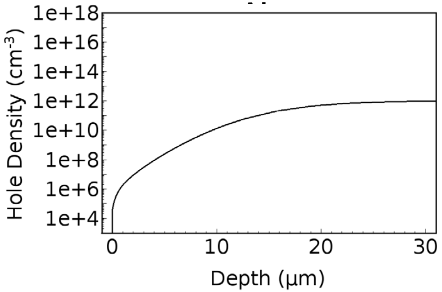

6" process.

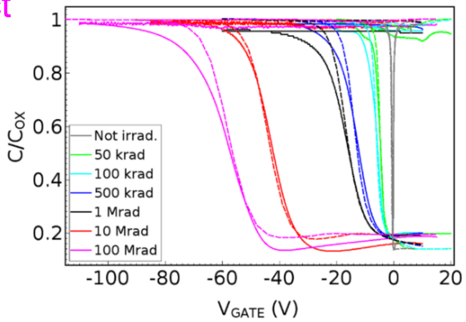

8" process.

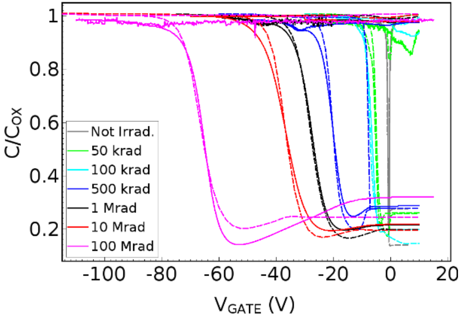

HPK MOS Capacitors

p-stop process.

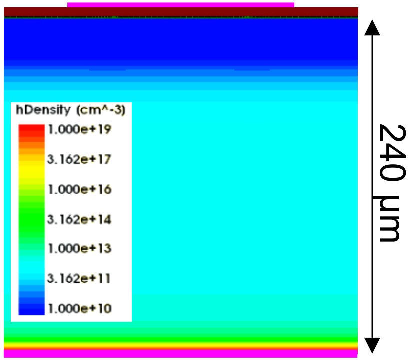

p-stop

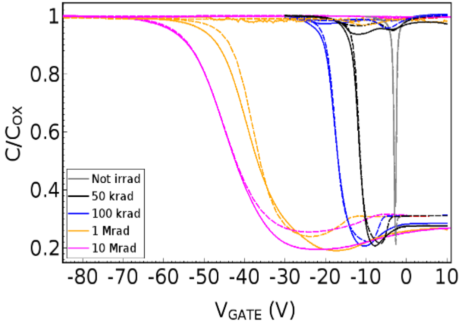

p-spray process.

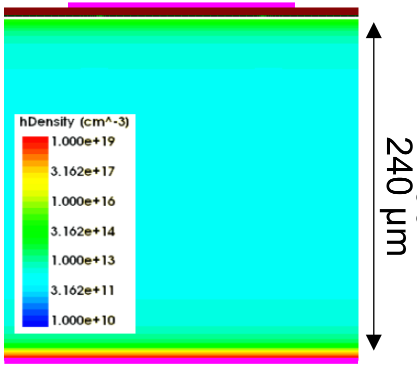

p-spray

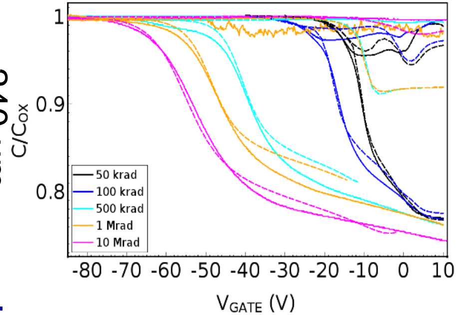

arianna.morozzi@pg.infn.it

Surface & Bulk model validation

Measurements
Simulations

HPK Gated Diodes

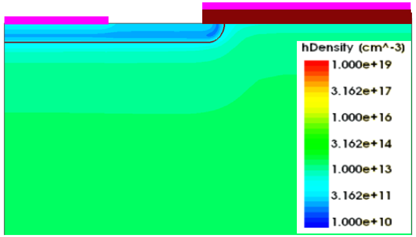

- ✓ I-V characteristics as a function of V_{GATE}.
- ✓ From I-V measurements the surface velocity s_0 was evaluated as a function of the dose.

$$s_0 = \frac{\pi}{2}\sigma_s v_{th} D_{it} k_B T \qquad s_0 = \frac{I_s}{n_i q A_G}$$

p-stop

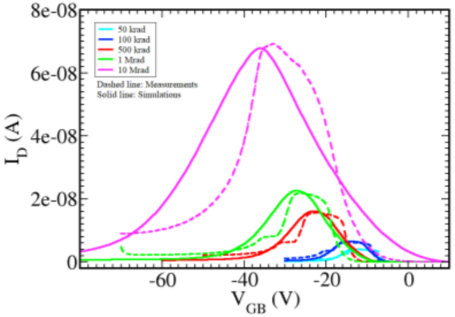

p-spray

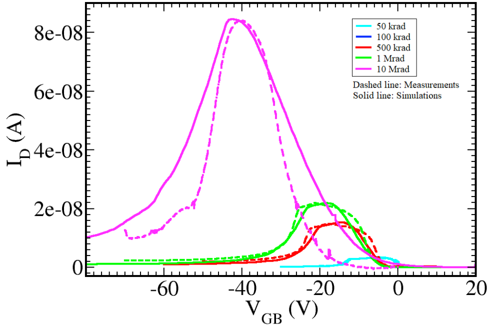

Charge Collection for silicon strips.

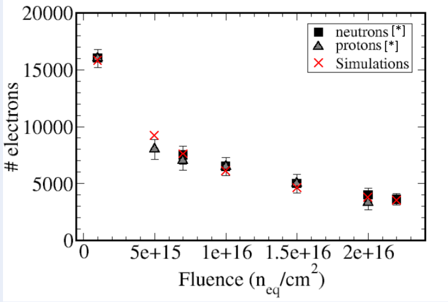

[*] A. Affolder et al., NIMA Vol. 623 (2010), pp. 177-179.

Charge Collection for PiN diodes.

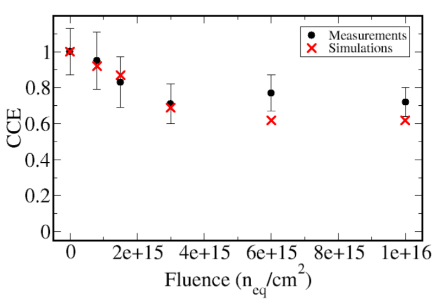

F. Moscatelli et al., IEEE TNS 64(8) (2017), pp. 2259 – 2267.
Data from M. Ferrero, 34th RD50 Workshop (2019)

INFN arianna.morozzi@pg.infn.it

PRELIMINARY

Deep Level Transient Spectroscopy

- **Defect spectroscopy**: *setup*, *training* and *measurements* at Deep Level Transient Spectroscopy (**DLTS**) system – SSD Lab, CERN EP-DT group (April-September ’25).

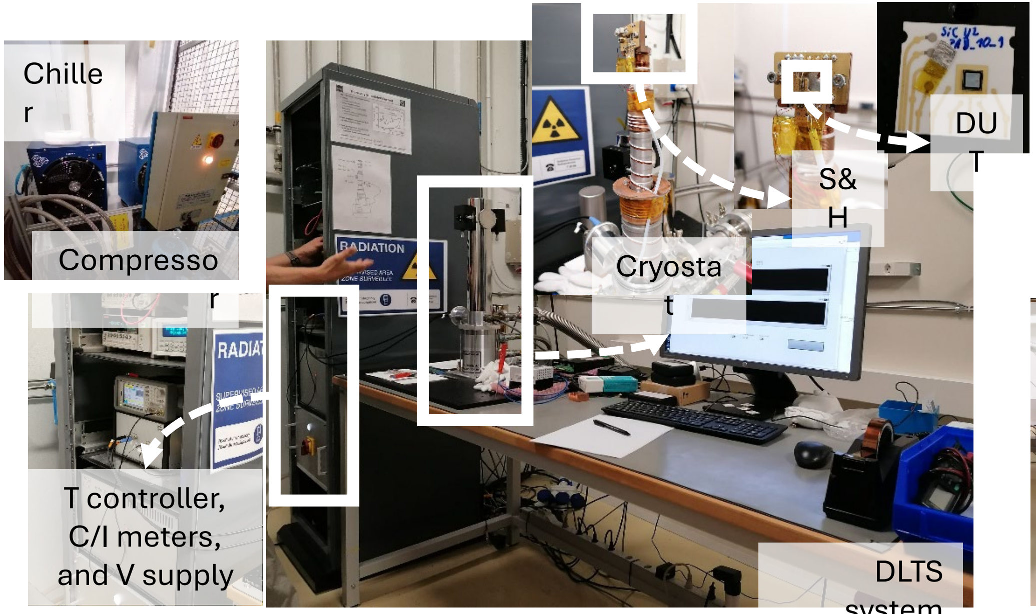

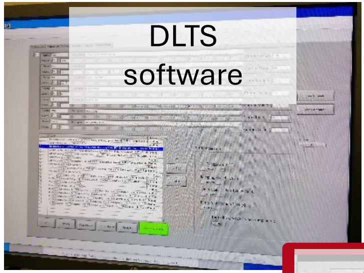

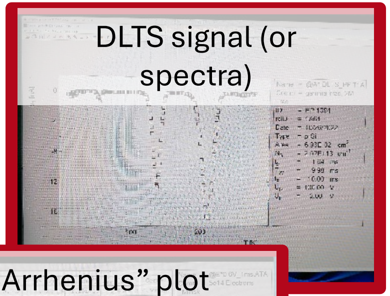

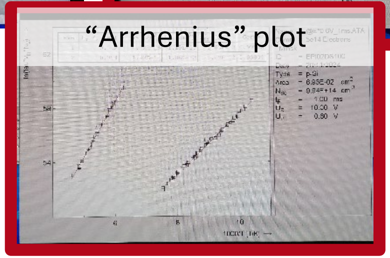

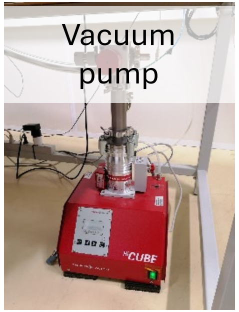

Defect parameters:
N_t, E_a and $\sigma_{e,h}$

PRELIMINARY

Deep Level Transient Spectroscopy: TCAD approach

- **Development** of a **TCAD simulation framework** capable of **reproducing** the **DLTS measurement results** – SSD Lab, CERN EP-DT group (April-September ’25).

Layout and Doping Concentration

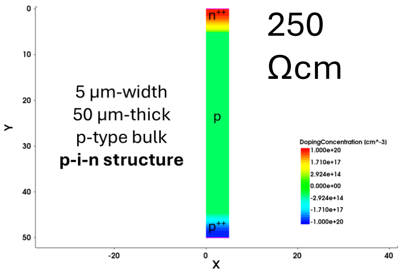

Majority Carrier Density

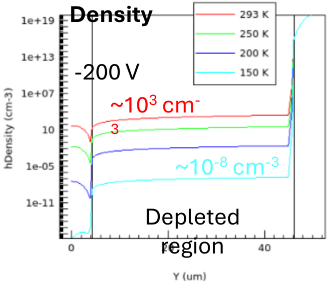

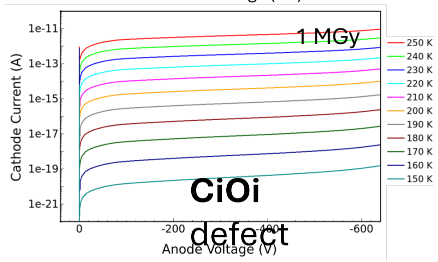

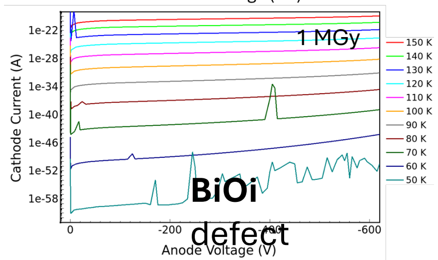

Example: BiOi defect @ 1 MGy

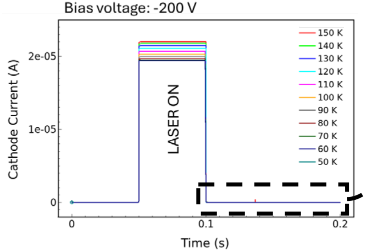

ZOOM

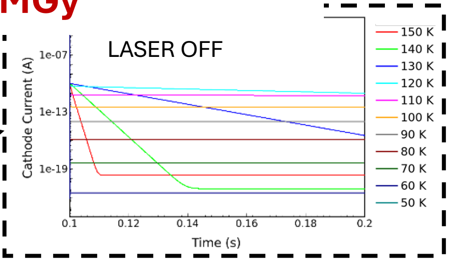

“Double Boxcar” Method

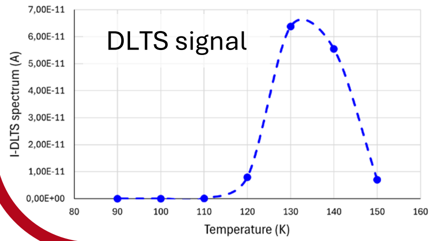

“Correlator Function” Method

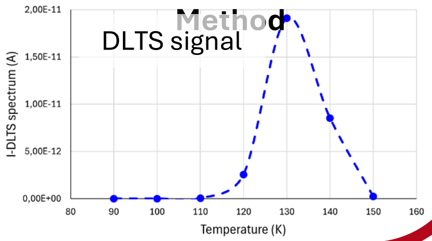

Silicon solid-state detectors

LGAD

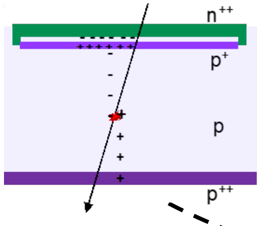

DC-RSD LGAD

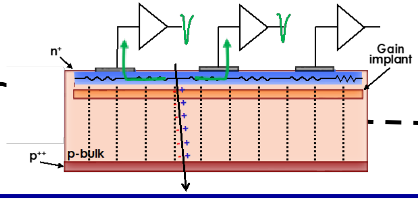

Compensated LGAD

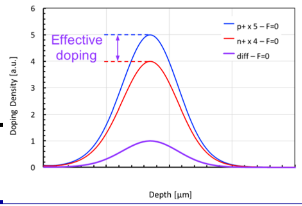

Monolithic CMOS pixel sensors

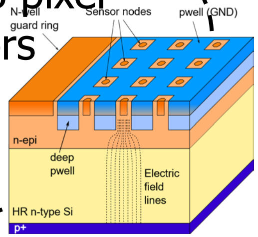

Silicon solid-state detectors

LGAD

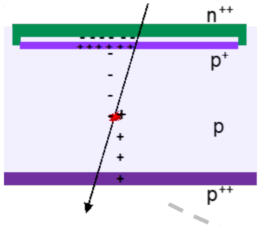

DC-RSD LGAD

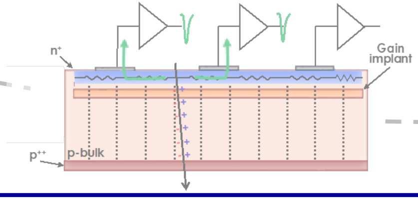

Compensated LGAD

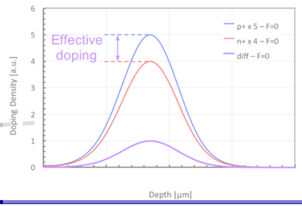

Monolithic CMOS pixel sensors

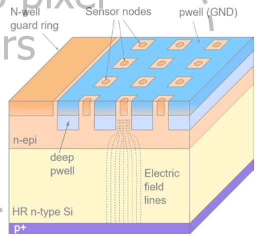

Low Gain Avalanche Diodes

This work has been supported by the Italian PRIN MIUR 2017 "4DInSiDe" under GA No 2017L2XKTJ, by the European Union's Horizon 2020 Research and Innovation programme under GA No 101004761 "eXFlu-innova" and it has been conducted in collaboration with the INFN CSN5 "eXFlu" research project.

- **Low-Gain Avalanche Diode (LGAD)**
  - **n-in-p silicon** sensors
  - Operated in **low-gain regime** (20 – 30)
  - **Critical electric field ~ 20 – 30 V/µm**
  - Good candidates for **4D tracking**
  - Mitigation of the radiation damage effects by exploiting the **controlled charge multiplication** mechanism.

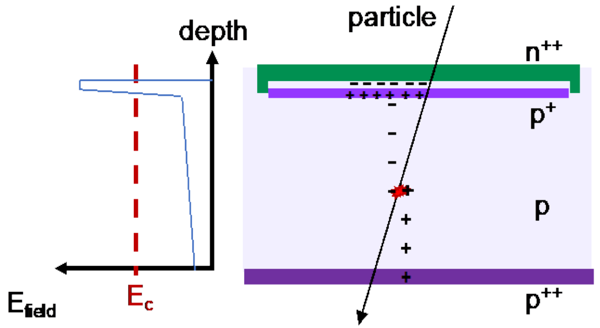

- **Advanced TCAD** modeling
  - **Radiation damage effects** model implementation
  - Accounts for the acceptor removal mechanism[5] which deactivates the p⁺-doping of the gain layer with irradiation.
  - Electrical behavior **prediction/ performance optimization** up to the highest fluences.

Layout and **doping profile**

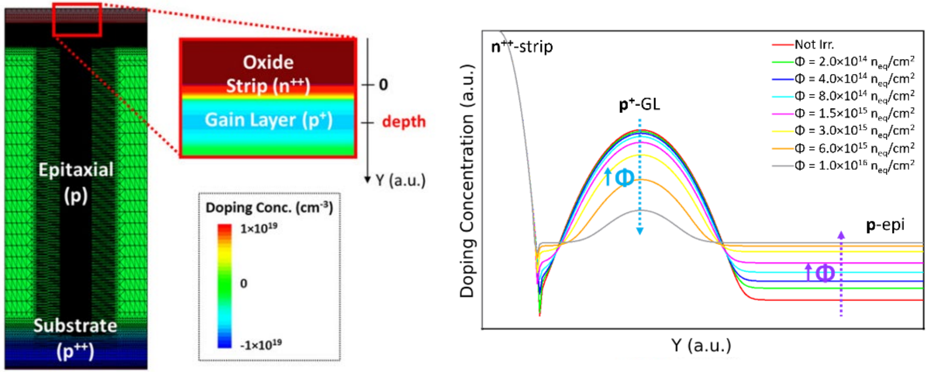

M. Ferrero et al., doi:10.1016/j.nima.2018.11.121
T. Croci et al 2022 JINST 17 C01022

Gain layer sensitivity analysis

This work has been supported by the Italian PRIN MIUR 2017 "4DInSiDe" under GA No 2017L2XKTJ, by the European Union's Horizon 2020 Research and Innovation programme under GA No 101004761 "eXFlu-innova" and it has been conducted in collaboration with the INFN CSN5 "eXFlu" research project.

- Three different doping profiles considered
  - Shallow, Standard, Deep.
  - **Gain layer** peak: a variation of a few percentages affects the breakdown voltage (V_{BD}).
  - Effect on the gain layer depletion voltage.
  - **Predictive** analysis on sensor performance considering the **radiation damage effects**.

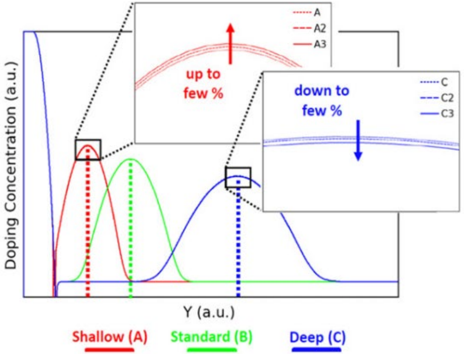

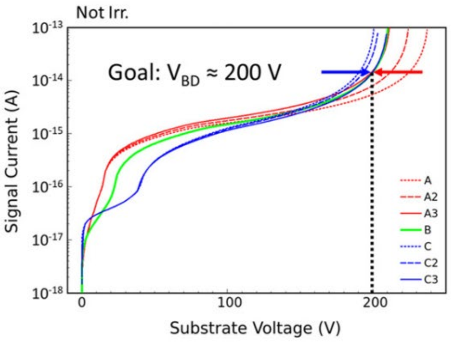

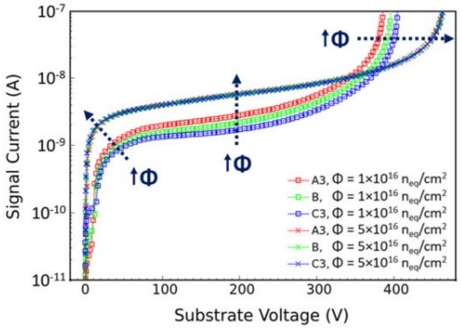

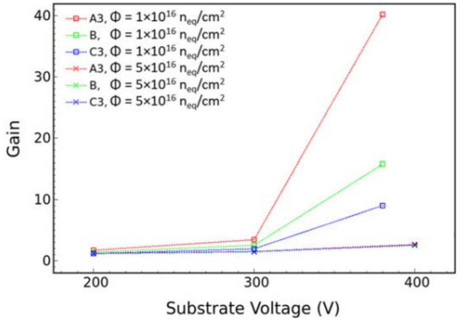

T. Croci et al 2023 JINST 18 C01008.

arianna.morozzi@pg.infn.it

LGAD: Electrical behavior investigation

This work has been supported by the Italian PRIN MIUR 2017 "4DInSiDe" under GA No 2017L2XKTJ, by the European Union's Horizon 2020 Research and Innovation programme under GA No 101004761 "eXFlu-innova" and it has been conducted in collaboration with the INFN CSN5 "eXFlu" research project.

- **FBK LGADs** (UFSD2, W1)
  - 55 μm thick
- **HPK LGADs** (HPK2, split 1-2)
  - 50 μm thick
- Simulations-Measurements comparison for not irradiated and irradiated devices.
- TCAD settings:
  - "PerugiaModDoping"
  - Massey avalanche model (FBK) and vanOverstraeten-de Man (HPK).
  - Temperature sets as per experimental measurements (RT not irrad, 248 K irrad).

FBK LGADs

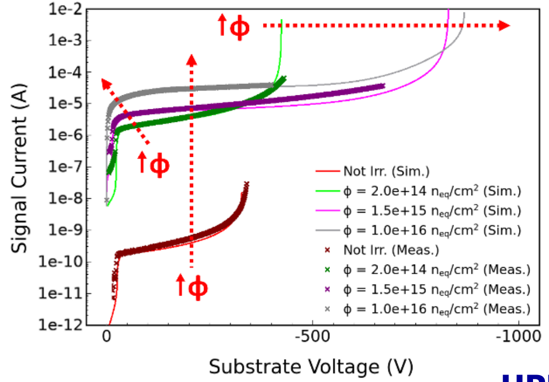

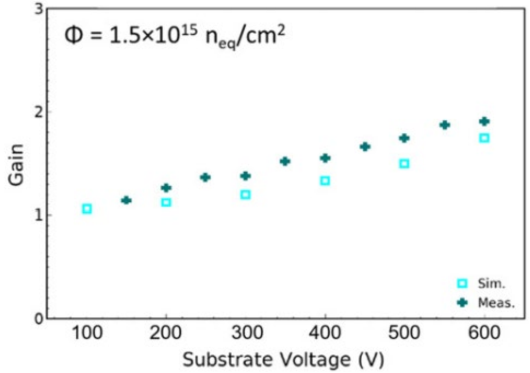

HPK LGADs

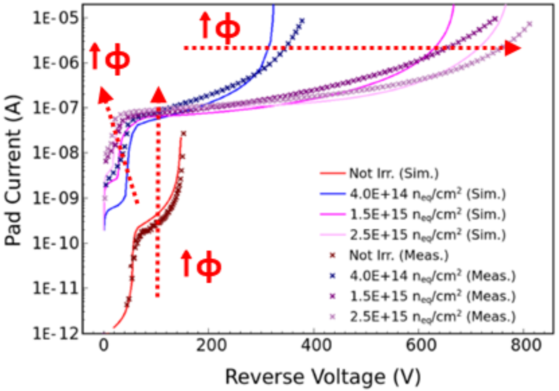

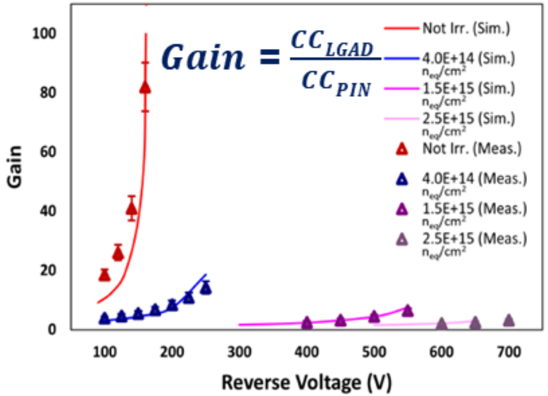

arianna.morozzi@pg.infn.it

Silicon solid-state detectors

LGAD

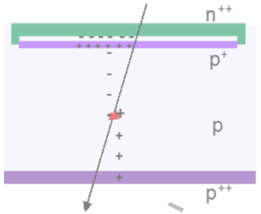

DC-RSD LGAD

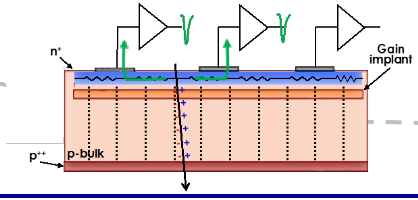

Compensated LGAD

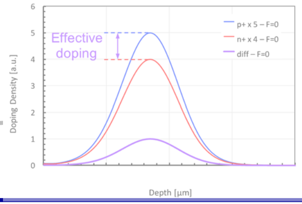

Monolithic CMOS pixel sensors

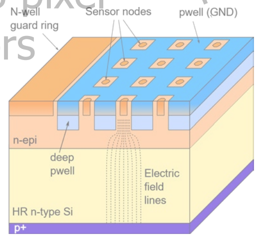

arianna.morozzi@pg.infn.it

Resistive Silicon Detectors (RSDs)

AC-RSD LGAD

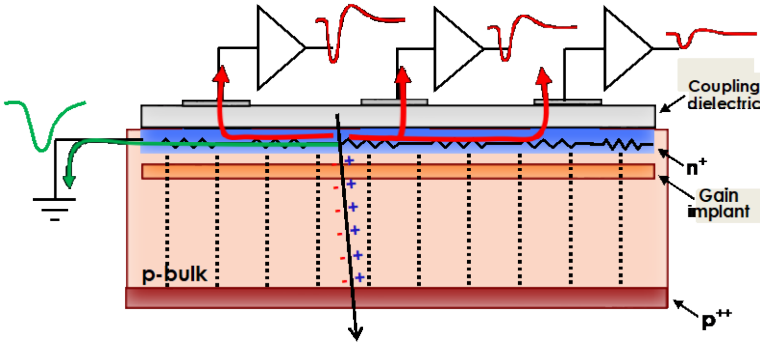

- ✓ This design has been manufactured in several productions by FBK, BNL, and HPK.

1. Long-tail bipolar signals
2. Baseline fluctuation
3. Uncontrolled signal spreading
4. Not easily scalable to large-area sensors

R. Arcidiacono et al., NIM A 1057 (2023), 168671

DC-RSD LGAD

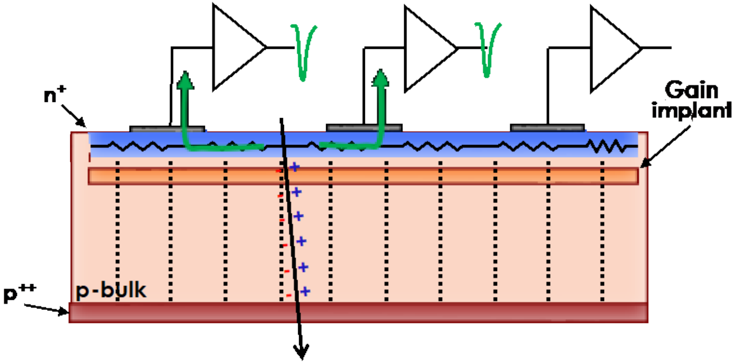

- ✓ Design actually under development by FBK.
- ✓ Promising solution for 4D tracking.

1. Unipolar signals
2. Absence of baseline fluctuation
3. Controlled signal spread
4. Large sensitive areas

- ✓ Evaluation of different layouts and technologies for future DC-RSD production using TCAD tools;

Heavy Ion model description

- Transient time simulation to study the active behavior of detectors.

- HeavyIon model.

```
HeavyIon(
  Time = 1e-9
   Location =(0,0)
   Direction =(0,1)
   Let_f = @LET_f_pC@
   Length = 60
   Wt_hi = 0.25
   Picocoulomb)
```

- After the heavy ion impinges the device across a specified particle path, electron-hole pairs are generated and by means of drift-diffusion mechanisms reach the collect contacts.

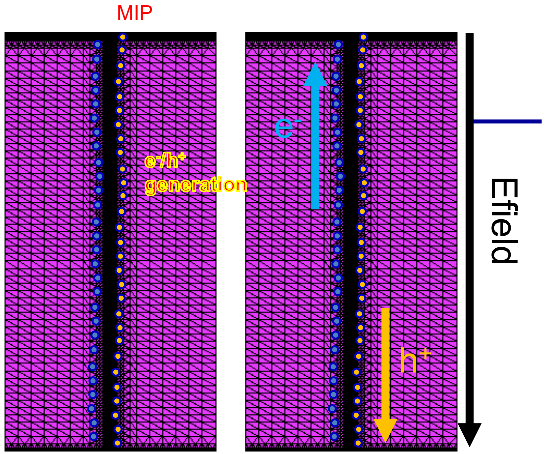

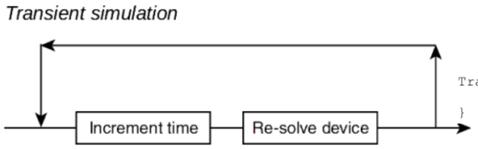


```
Transient( InitialTime = 0.0 FinalTime=1.0e-5 ){
   Coupled { Poisson Electron Hole }
}
```

Reconstruction

- ✓ Stimulus MIP (Minumum Ionizing particle)
- ✓ The position is reconstructed using the charge imbalance

$$x_i = \frac{Q_{top\ right} + Q_{bottom\ right} - Q_{top\ left} - Q_{bottom\ left}}{Q_{tot}}$$

$$z_i = \frac{Q_{top\ right} + Q_{top\ left} - Q_{bottom\ left} - Q_{bottom\ right}}{Q_{tot}}$$

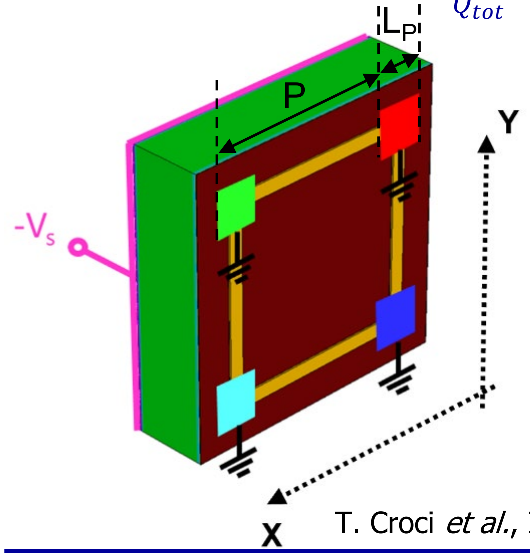

L_P = 15 µm

P = 105 µm

@ V_{Back} = -110 V

$R_{s,n++} \approx 721\ \Omega_{sq}$

$R_{s,strip} \approx 15\ m\Omega/\mu m$

T. Croci *et al.*, IEEE TNS (2024) 3356826.

Results from *TCAD* simulations

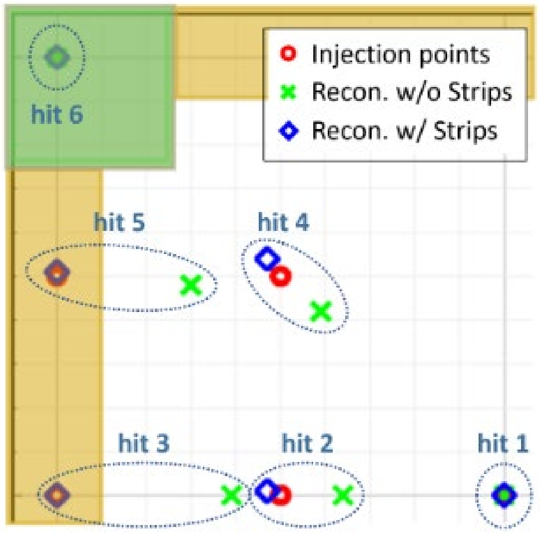

Avalanche model: **Massey**. Temperature **300 K**

Investigate the effect of the contact resistance

- Investigation of the signal confinement within the TCAD environment.
- Minimum Ionizing Particle (MIP): various hit points considered.

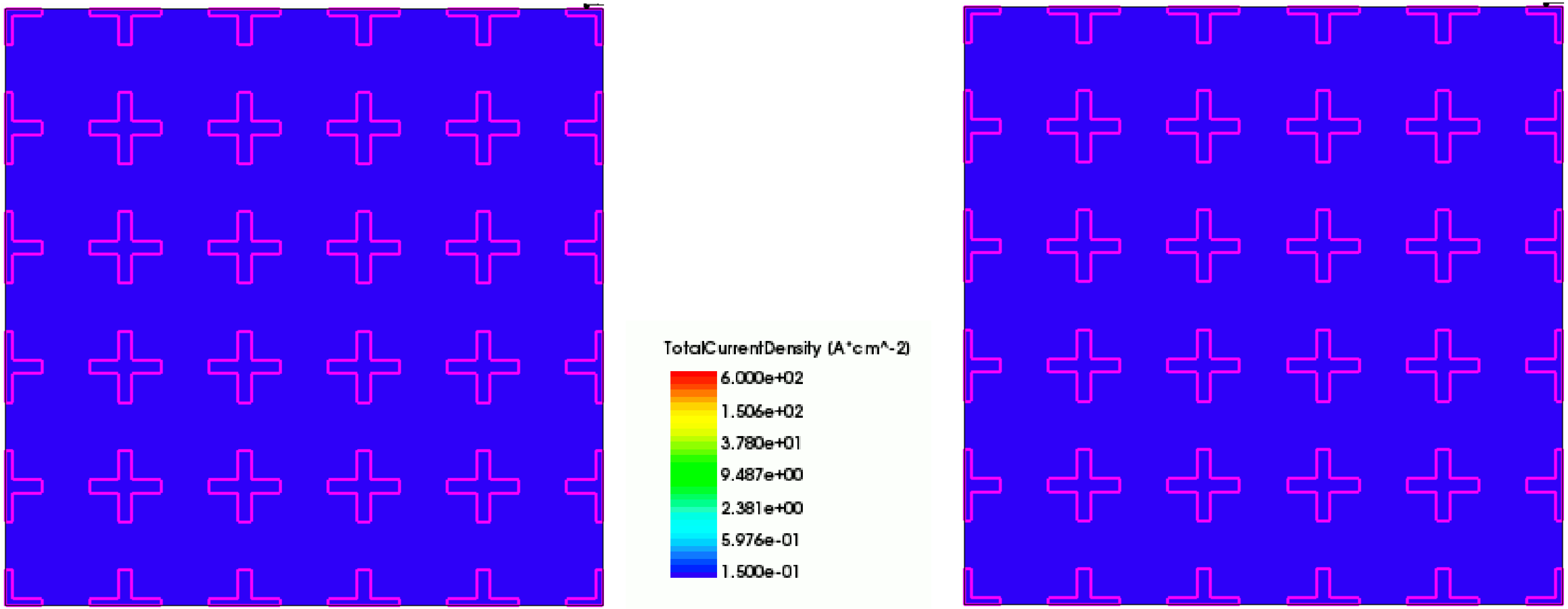

Contact resistance = $10\ \Omega$

Contact resistance = $1\ k\Omega$

arianna.morozzi@pg.infn.it

Investigate the effect of the contact shape

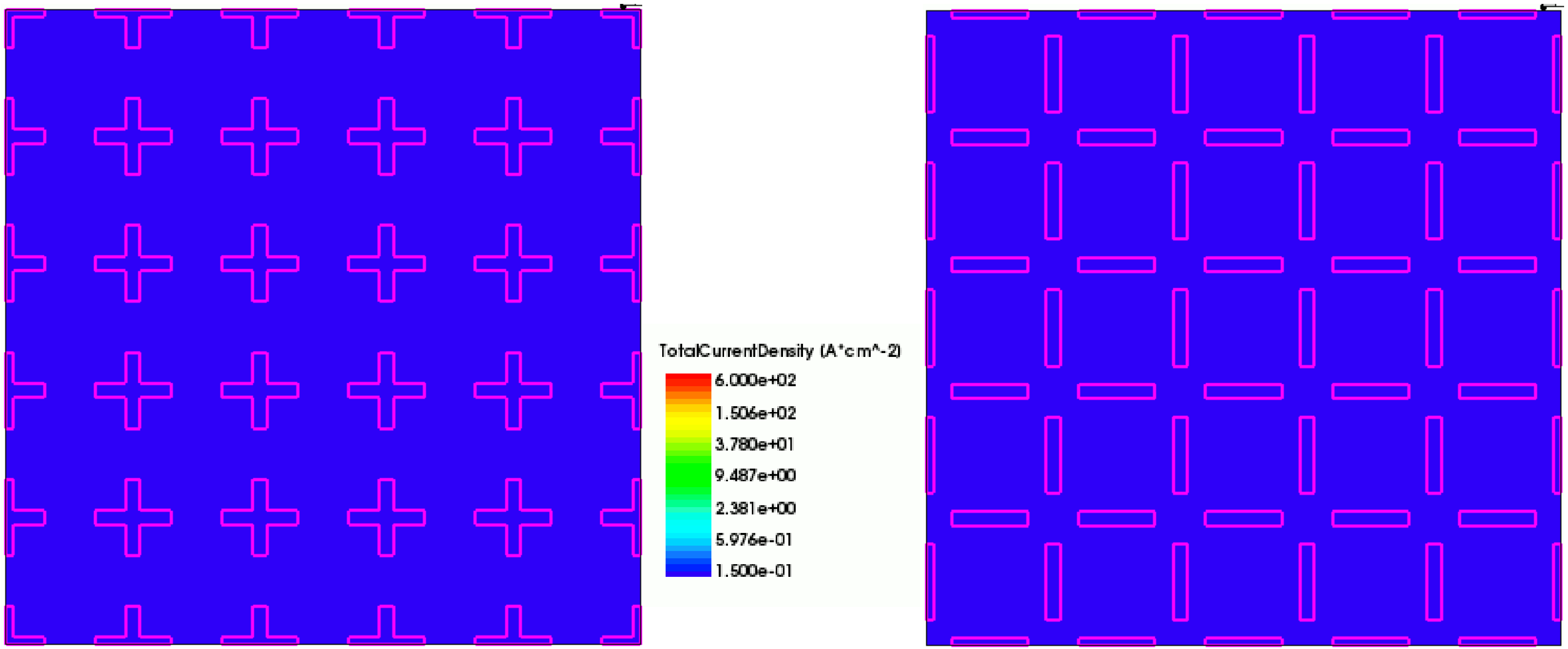

36 electrodes

60 electrodes

arianna.morozzi@pg.infn.it

Silicon solid-state detectors

LGAD

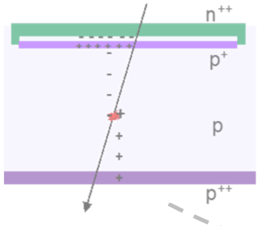

DC-RSD LGAD

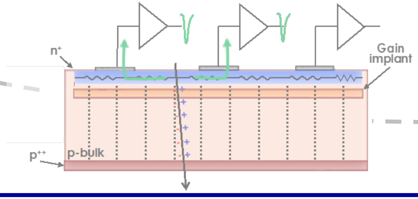

Compensated LGAD

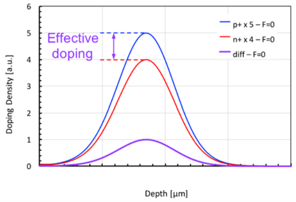

Monolithic CMOS pixel sensors

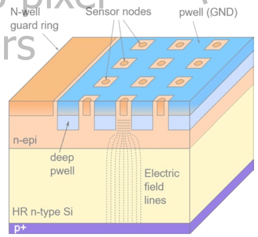

Compensated LGADs for eXtreme Fluences

Funded by the European Union

European Research Council

Doping Profile – Standard LGAD

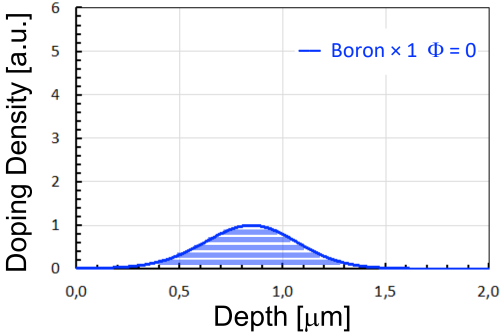

Irradiation

$\Phi = 1\times10^{16}/cm^2$

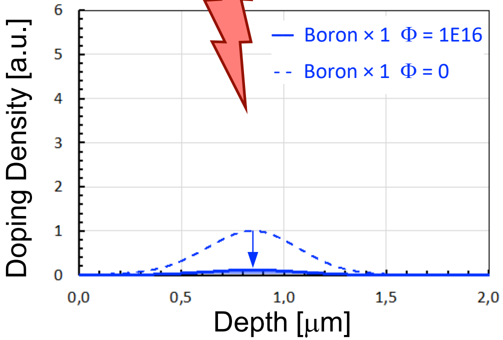

Doping Profile – Compensated LGAD

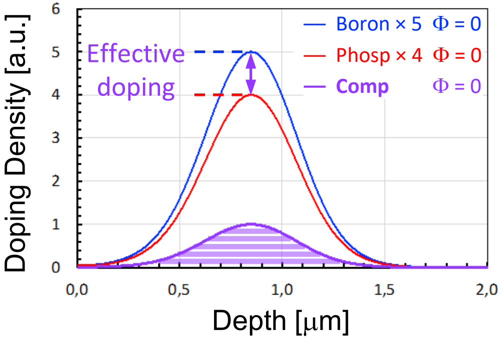

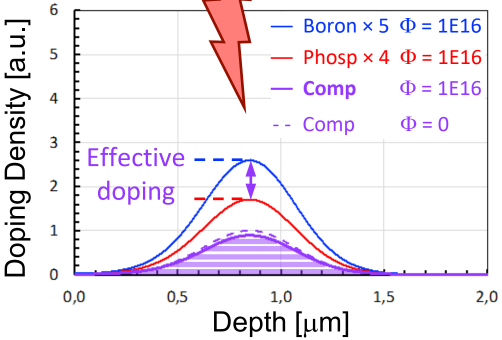

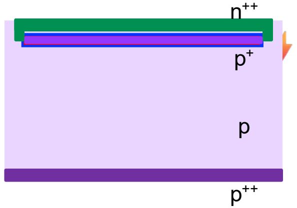

Compensated LGAD

Use the interplay between acceptor and donor removal to keep a constant gain layer active doping density

Many unknowns:

- ▻ donor removal coefficient, from $n^+(\Phi) = n^+(0)\cdot e^{-c_D\Phi}$
- ▻ interplay between donor and acceptor removal (c_D vs c_A)
- ▻ effects of substrate impurities on the removal coefficients

Material courtesy of V. Sola

INFN arianna.morozzi@pg.infn.it

Gain Removal Mechanism in LGADs

The acceptor removal mechanism deactivates the p^+-doping of the **gain implant** with irradiation as

$$p^+(\Phi) = p^+(0)\cdot e^{-c_A\Phi}$$

where c_A is the acceptor removal coefficient and depends on the initial acceptor density, $p^+(0)$, and on the defect engineering of the gain layer atoms

To substantially reduce c_A, it is necessary to increase $p^+(0)$, the initial acceptor density

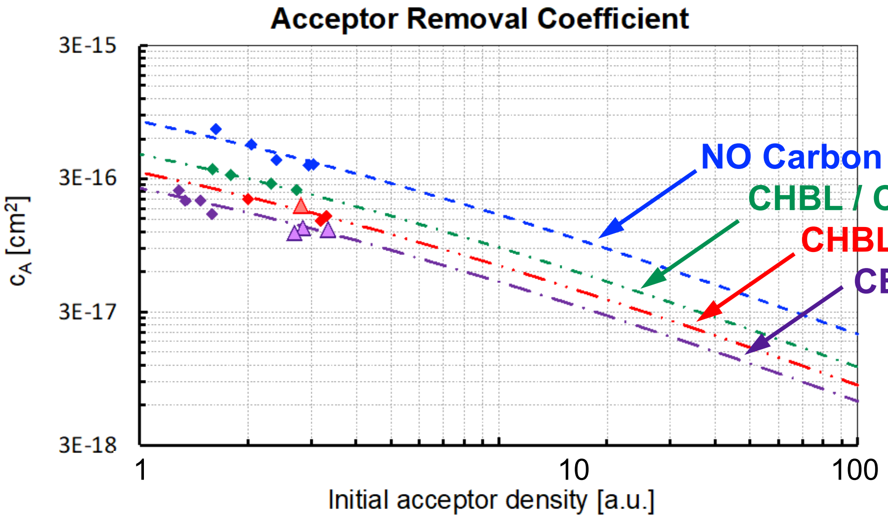

▲ thin sensors from the EXFLU1 batch

[R.S. White, 43rd RD50 Workshop (2023) CERN]

Gain Removal Mechanism in LGADs

The acceptor removal mechanism deactivates the p⁺-doping of the **gain implant** with irradiation as

$$p^+(\Phi) = p^+(0)\cdot e^{-c_A\Phi}$$

where c_A is the acceptor removal coefficient and depends on the initial acceptor density, $p^+(0)$, and on the defect engineering of the gain layer atoms

To substantially reduce c_A, it is necessary to increase $p^+(0)$, the initial acceptor density

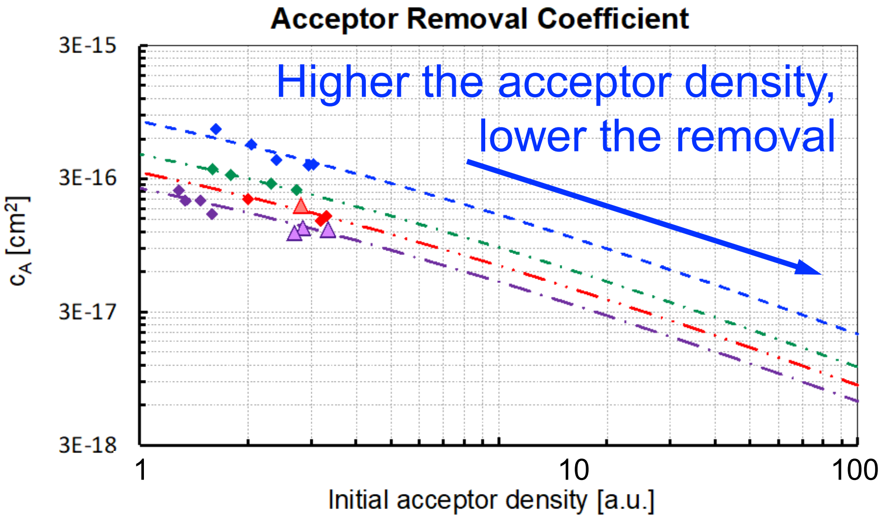

▲ thin sensors from the EXFLU1 batch
[R.S. White, 43rd RD50 Workshop (2023) CERN]

arianna.morozzi@pg.infn.it

Investigation of the donor removal

While donor removal has been investigated for doping densities of $10^{12} – 10^{14}$ cm^{-3}, the design of compensated LGADs requires examining the $10^{15} – 10^{17}$ cm^{-3} range, which will be addressed through two different methodologies.

Comparison between TCAD simulations and experimental measurements of

compensated LGADs (C-V) **&** **van der Pauw test structures (R_{sh})**

EXFLU1's split table

[a < b < c]

[2c < 3a]

Wafer #	Thickness	p+ dose	n+ dose	C dose
6	30	2 a	1	
7	30	2 b	1	
8	30	2 b	1	
9	30	2 c	1	
10	30	3 a	2	
11	30	3 b	2	
12	30	3 b	2	
13	30	3 b	2	1.0
14	30	3 c	2	
15	30	5 a	4	

A.Fondacci

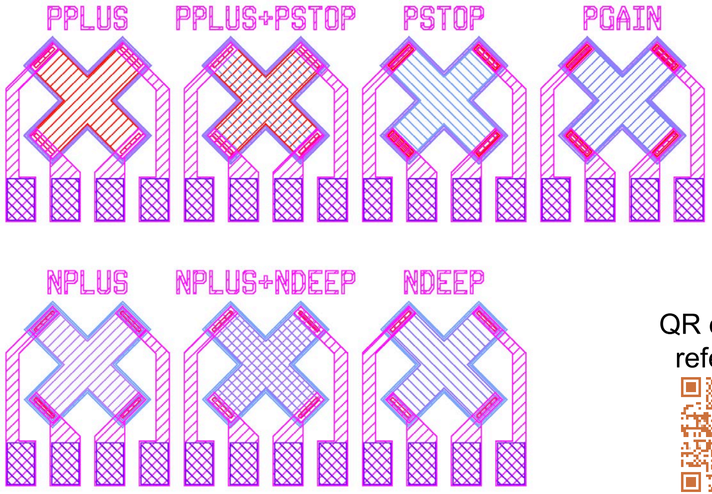

QR code for reference

arianna.morozzi@pg.infn.it

Compensated LGADs to extract donor removal

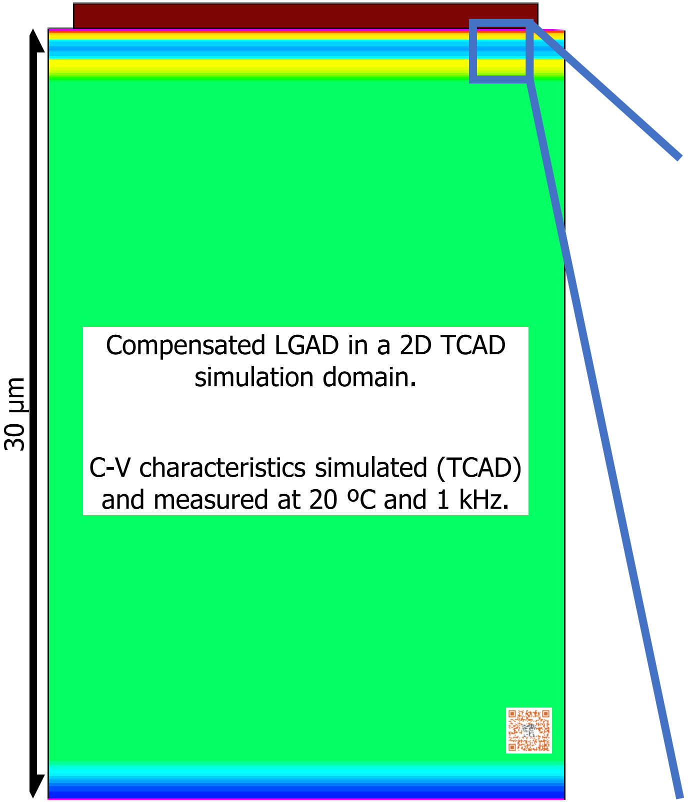

Compensated LGAD in a 2D TCAD simulation domain.

C-V characteristics simulated (TCAD) and measured at 20 ºC and 1 kHz.

A.Fondacci

arianna.morozzi@pg.infn.it

Compensated LGADs to extract donor removal

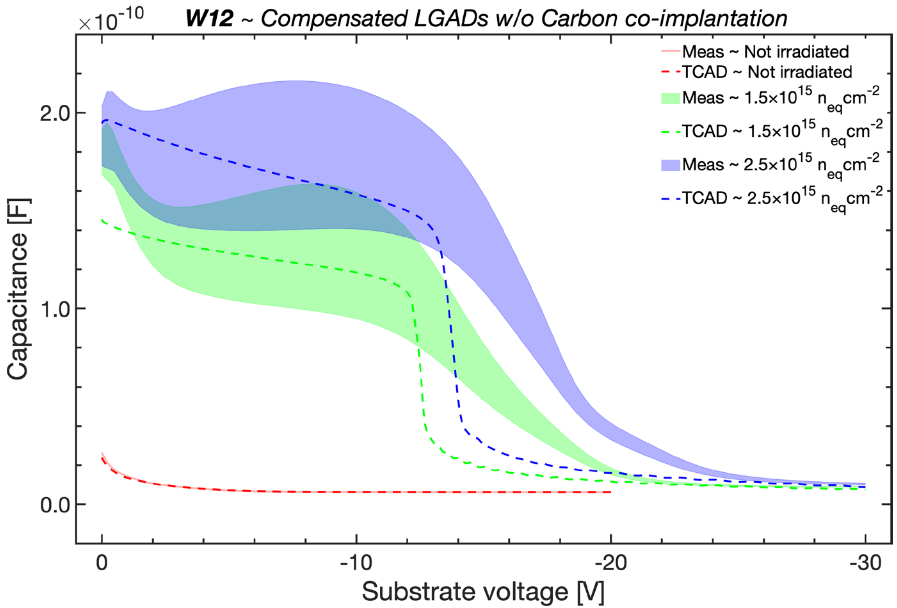

Exploiting the experimental acceptor removal coefficient **c_A = 2.50·10^{-16} cm²**, the agreement with C-V measurements is achieved using a donor removal coefficient **c_D = 6.50·10^{-16} cm²**.

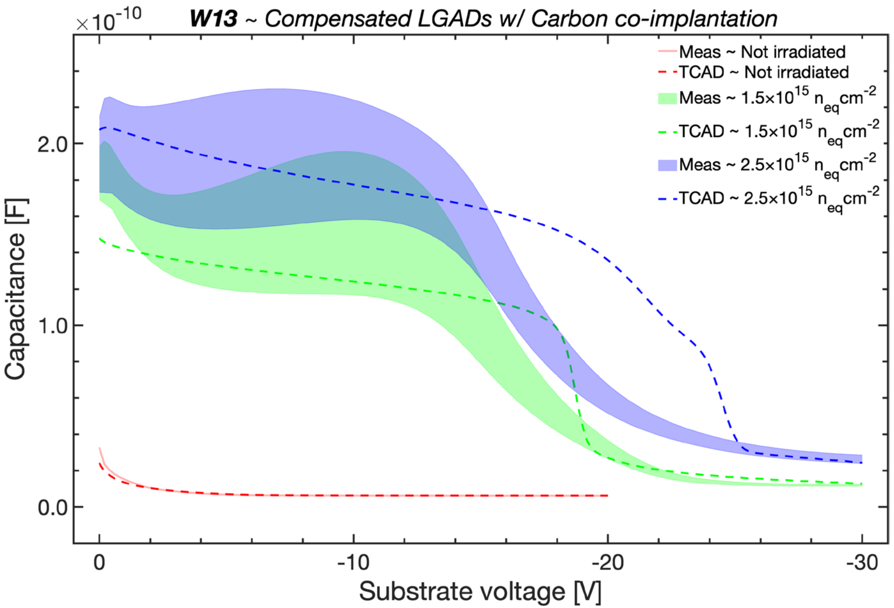

Exploiting the extracted **c_D = 6.50·10^{-16} cm²** and the experimental **c_A = 8.26·10^{-17} cm²** for carbon co-implantation, a good agreement between measurements and simulations was achieved.

A.Fondacci

arianna.morozzi@pg.infn.it

Van der Pauw TS to extract donor removal

Use of the variation in sheet resistance with irradiation to extract and validate donor (and acceptor) removal.

A.Fondacci

Van der Pauw TS to extract donor removal

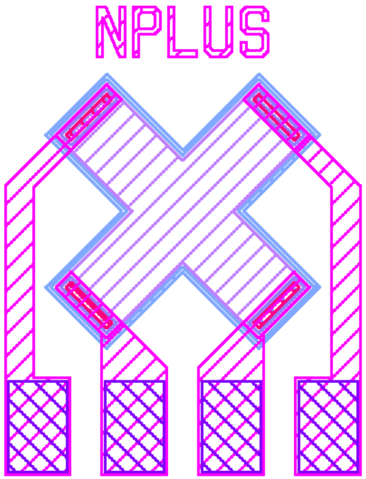

Merely out of curiosity

A.Fondacci

c_D donor removal coefficient values $[10^{-16}\ \mathrm{cm}^2]$				
Location	Irradiation	W3	W6	W14
KIT	Neutron	1.5 ± 0.2	1.0 ± 0.2	0.6 ± 0.2
	Proton	4.6 ± 0.4	2.9 ± 0.4	1.7 ± 0.3
Perugia	Neutron	1.6 ± 0.2	1.0 ± 0.2	0.7 ± 0.1
	Proton	4.7 ± 0.6	2.9 ± 0.4	1.7 ± 0.3

arianna.morozzi@pg.infn.it

Taking Stock

- Compensated LGADs aim to extend 4D tracking to the extreme fluences expected at future hadron colliders.
- Their design requires an accurate characterisation of donor removal at high initial donor concentrations ($>10^{15}$ cm^{-3}).
- To this end, two new strategies have been explored, leading to the following preliminary results:

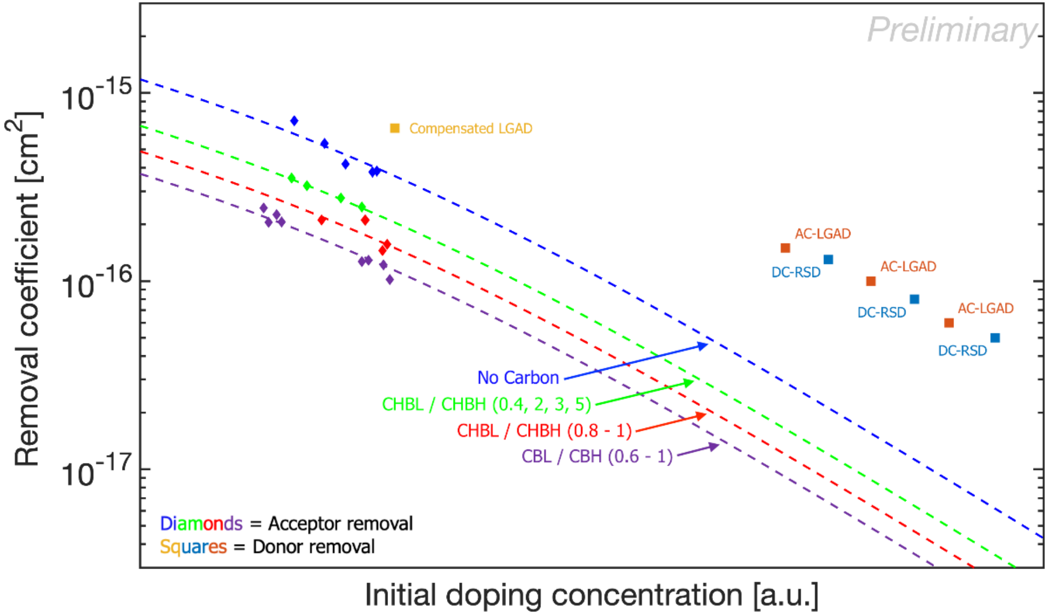

A.Fondacci

Silicon solid-state detectors

LGAD

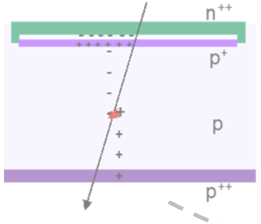

DC-RSD LGAD

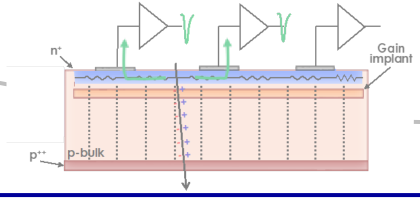

Compensated LGAD

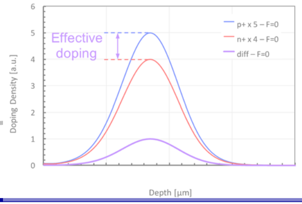

Monolithic CMOS pixel sensors

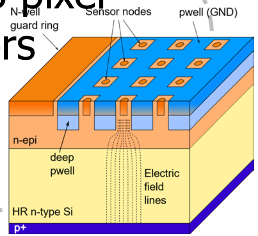

arianna.morozzi@pg.infn.it

Monolithic sensors with avalanche gain

Main driver: **ALICE 3 ToF layers.** Target resolution: 20ps

Fully Depleted PAD sensors

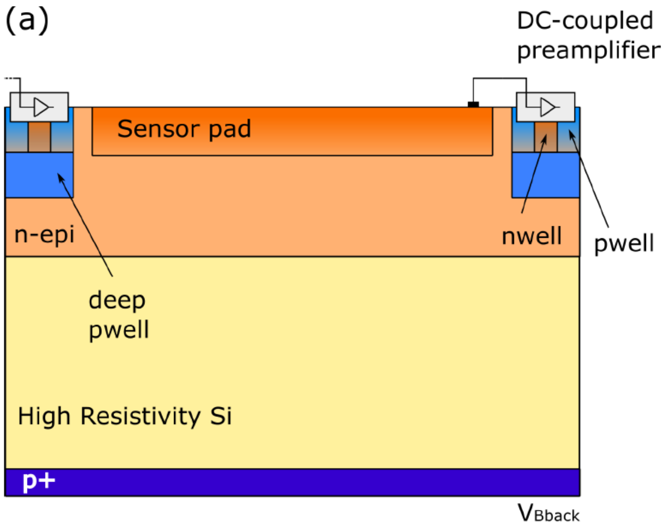

- Sensors can be biased at low voltage
- DC coupling with front-end amplifier is possible

Fully Depleted PAD sensors with avalanche gain

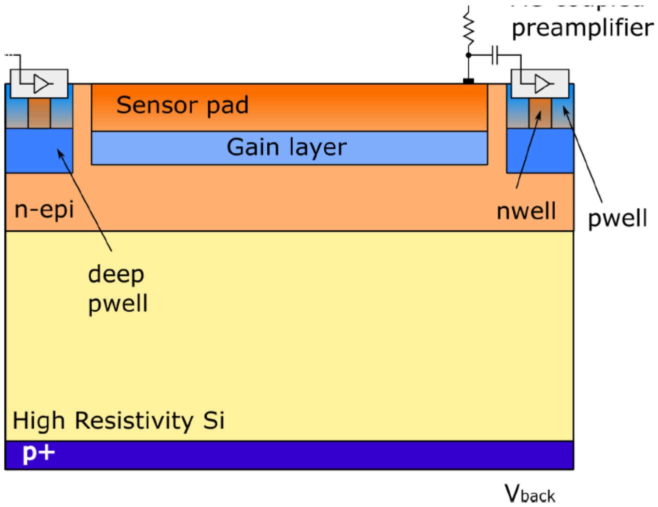

- High voltage is needed on the top side
- AC coupling of front-end amplifier is needed

Material courtesy of L. Pancheri (ICICDT2025)

Monolithic sensors with avalanche gain: junction termination

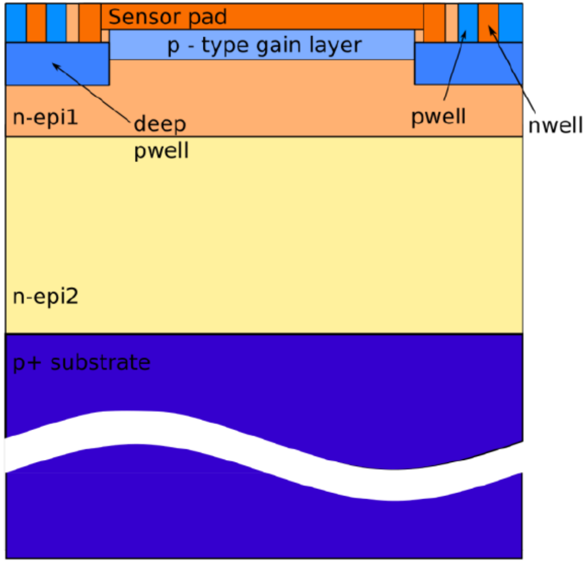

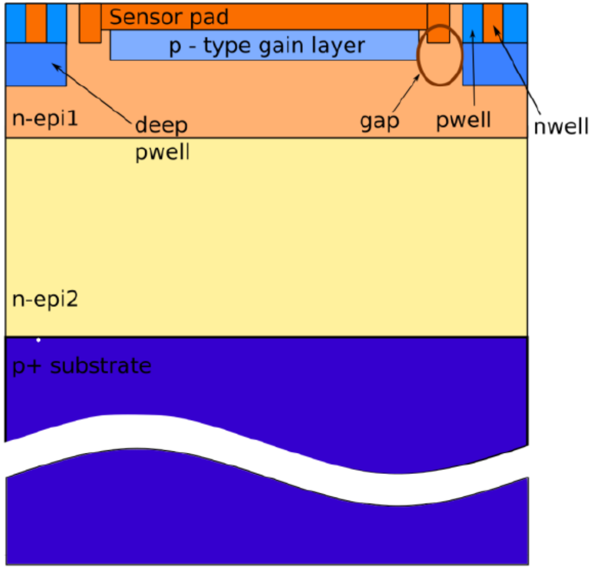

Layout A1

Termination shielded by deep pwell: electrons generated below the deep pwell reach the gain layer

Layout A2

Termination directly **facing the active region**: electrons generated below termination can be collected without gain

Material courtesy of L. Pancheri (ICICDT2025)

arianna.morozzi@pg.infn.it

Monolithic sensors with avalanche gain: electric field lines

All the field lines cross the gain region:
- **100% fill factor**
- non-uniform gain and timing

Peripheral field lines don't cross the gain region:
- «dead area» at the borders with gain 1
- **better for timing** uniformity

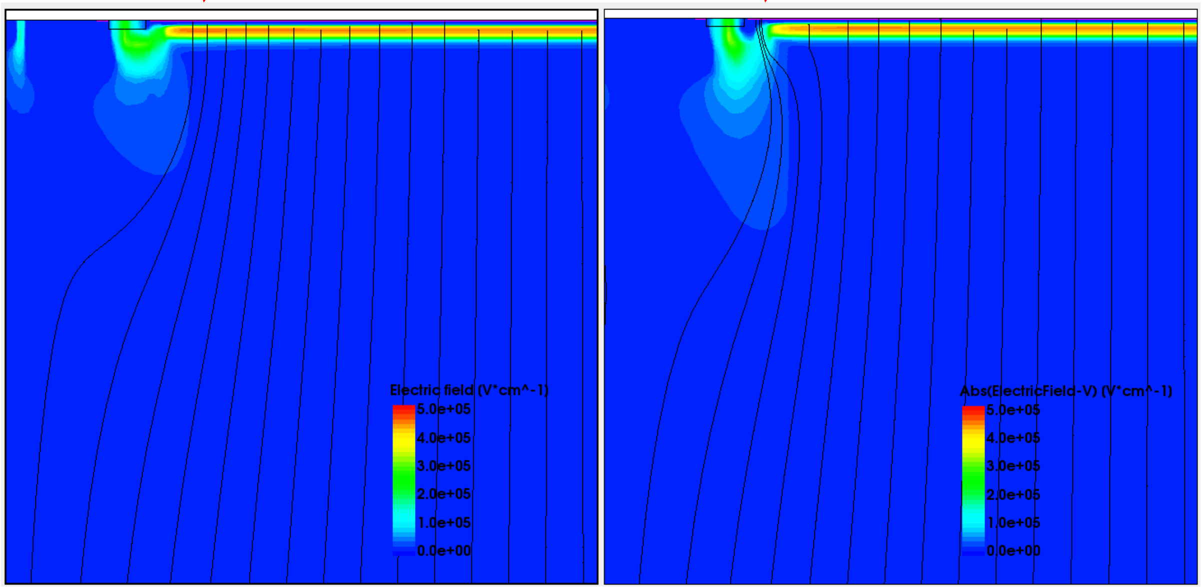

Layout A1

Layout A2

Material courtesy of L. Pancheri (ICICDT2025)

arianna.morozzi@pg.infn.it

Experimental results: gain and timing resolution

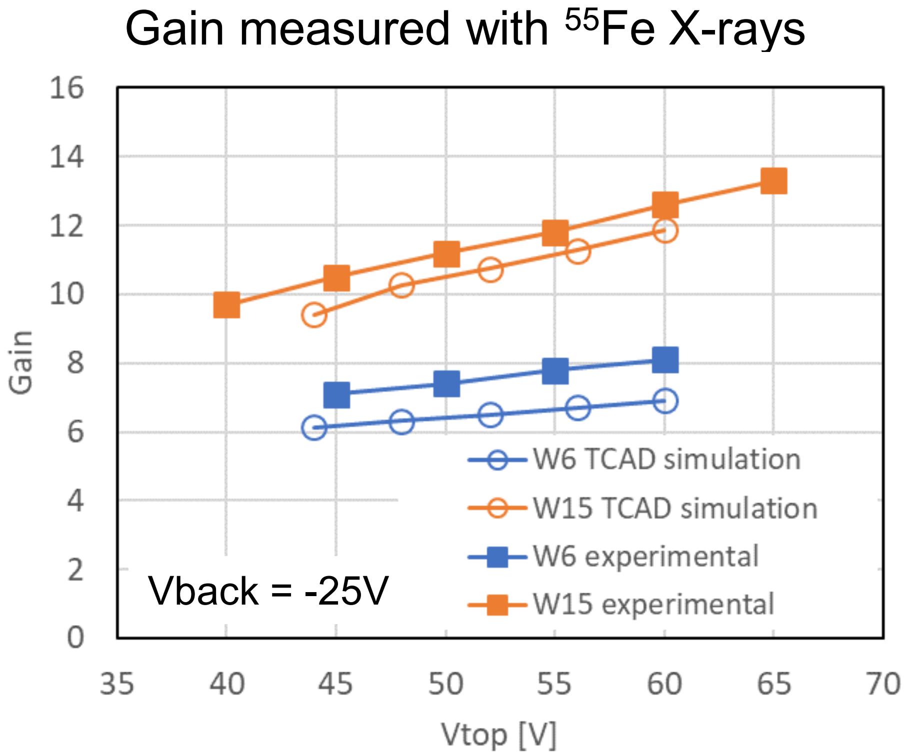

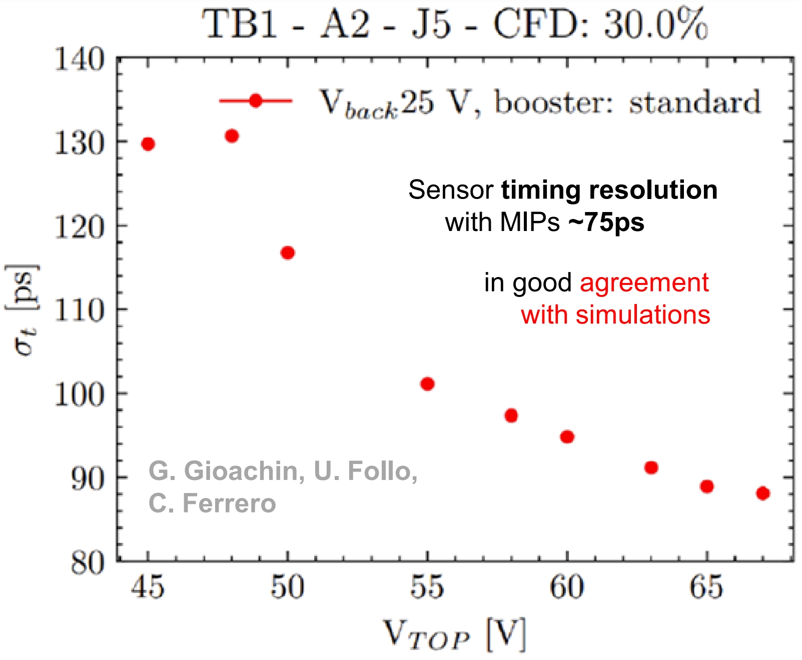

Fabrication run with **thinner active layers** and **higher gain** planned to further improve timing resolution

Material courtesy of L. Pancheri (ICICDT2025)

Rad-hard/Innovative materials

Diamond

SiC

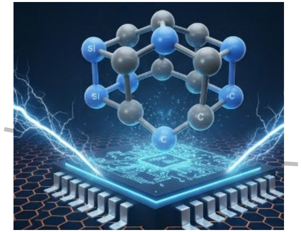

a:Si-H

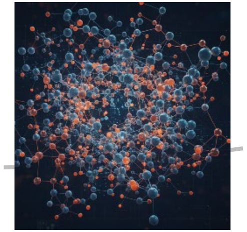

Ferroelectrics
NC-FETs

Rad-hard/Innovative materials

Diamond

SiC

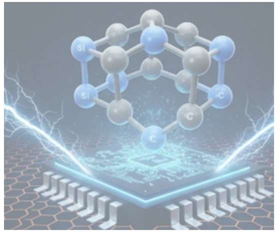

a:Si-H

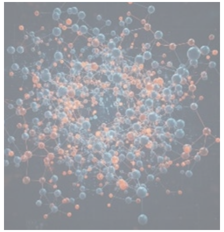

Ferroelectrics
NC-FETs

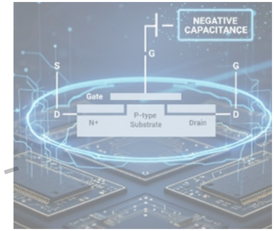

arianna.morozzi@pg.infn.it

CVD DIAMOND for particle detection applications

Silicon vs Diamond in **Electronics** (**radiation detection**)

	Silicon	Diamond	
Bandgap [eV]	1,12	5,47	**Higher-Field operation**
Breakdown Field [MV/cm]	0,4	20	
Intrinsic Resistivity@R.T. [Ω cm]	$2,3x10^{5}$	$> 10^{11}$	**lower leakage current**
Intrinsic Carrier Density [cm^{-3}]	$1,5x10^{10}$	10^{-27}	
Dielectric Constant	11,9	5,7	
Electron Mobility	1350	1900-3800	**faster signal**
Hole Mobility	480	2300-4500	
Saturation Velocity	$1x10^{7}$	$2,7x10^{7}$	
Displacement Energy [eV/atom]	13-20	43	**radiation hardness**
Thermal Condutivity [W cm^{-1} K^{-1}]	1,5	20	**heat dissipation**
Energy to create e-h pair [eV]	3,62	11,6 - 16	
Radiation Length [cm]	9,36	12,2	
Energy Loss for MIPs [MeV/cm]	3,21	4,69	
Aver. Signal Created / 100 µm	8892	3602	**lower signal**

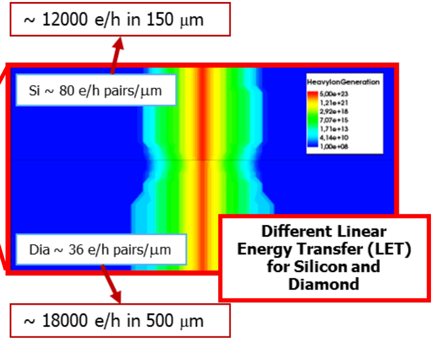

✓ Physically-based numerical model of Diamond

- fully implemented within the TCAD environment.
- Robust and reusable simulation framework.
- Only one fitting parameter (N_T) to reproduce the experimental behavior of diamond.
- Development of a physically based diamond numerical model (deep-level traps).
- CCE as validation figure of merit (comparison with experimental data).

CVD diamond

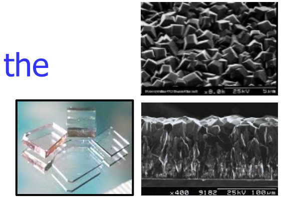

SEM images of a polycrystalline (pc) CVD diamond film: top view and cross section.

Synopsys© Sentaurus TCAD

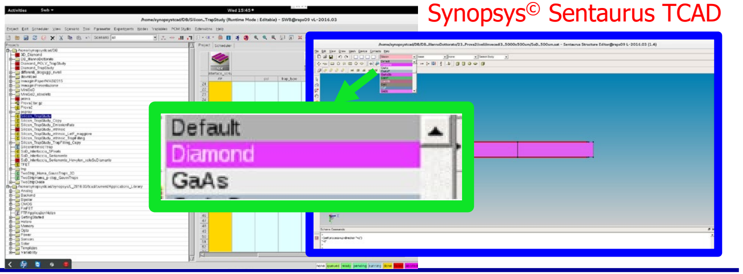

TCAD modeling of CVD DIAMOND

✓ Innovative diamond modeling for DC, TV analyses within Synopsys© Sentaurus TCAD

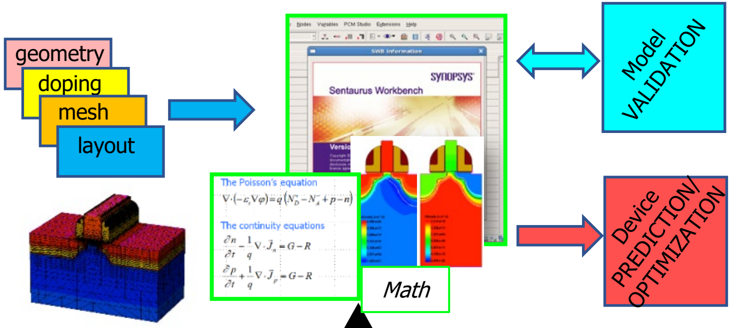

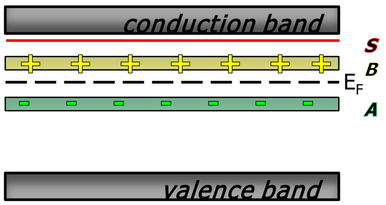

	Type	E (eV)	σ_e (cm^2)	σ_h (cm^2)	N_T (cm^{-3})
Level S	Donor	E_C - 0.05	$1\cdot10^{-13}$	$1\cdot10^{-18}$	$N_T/2$
Level B	Donor	E_C - 0.8	$1\cdot10^{-14}$	$1\cdot10^{-18}$	$N_T/2$
Level A	Acceptor	E_C - 2.7	$5\cdot10^{-16}$	$1\cdot10^{-13}$	N_T

CMOS Radiation Active Pixel Sensors (RAPS03) for particle detection
- ✓ UMC 0.18um 1P6M – no-epi layer
- ✓ Pixels (3T) with different layout options
- ✓ Thinned down to 20/25 µm

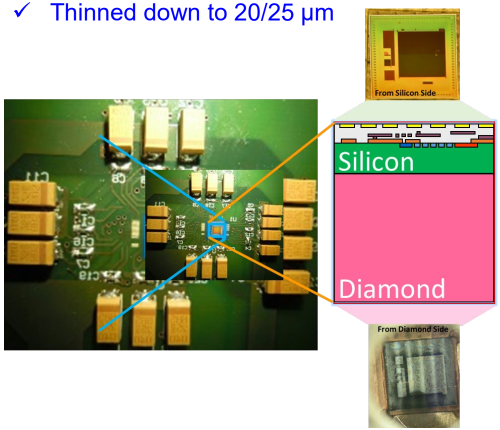

Transient Analysis

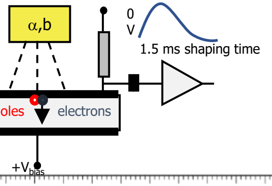

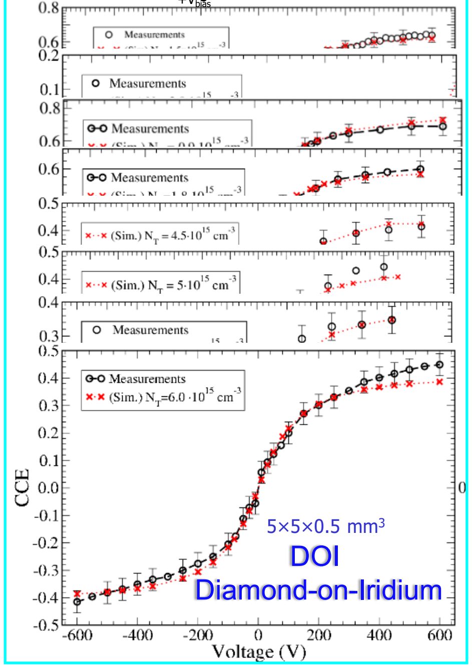

A. Morozzi et al., 13th Conference on Ph.D. Research in Microelectronics and Electronics (PRIME), pp. 73-76.
A. Morozzi et al., Materials Today: Proceedings, vol. 3, suppl. 2, 2016, pp. S153-S158, 2016.
A. Morozzi et al., JINST, 11, C12043, 2016.

arianna.morozzi@pg.infn.it

Rad-hard/Innovative materials

Diamond

SiC

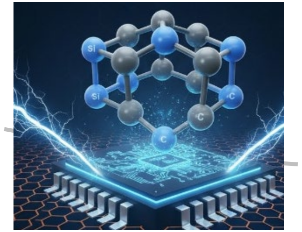

a:Si-H

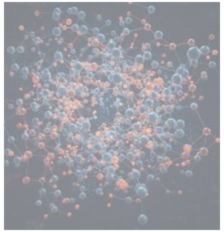

Ferroelectrics
NC-FETs

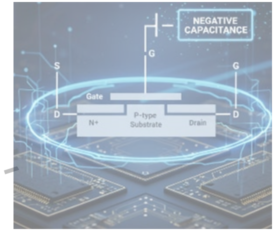

arianna.morozzi@pg.infn.it

Modeling SiC devices within the TCAD environment

ÖAW AUSTRIAN ACADEMY OF SCIENCES

Simulation setup

HEPHY INSTITUTE OF HIGH ENERGY PHYSICS

- Quasi - 1D simulation structure → fine mesh and fast simulation
- Adapted parameter file, strict convergence & error criteria [5]
- Assumed linear defect introduction with fluence and no intrinsic defects
- Initial parameters → Benchmark within the **wide** range of literature values
  Final parameters → Adapted to fit measurements

Defect	Type	Energy [eV]	σ_e [cm^2]	σ_h [cm^2]
Ti	Acceptor	Ec – (0.11 – 0.23) [7, 9, 13, 17, 23, 27]	$3.0 \cdot 10^{-18} - 4.0 \cdot 10^{-13}$ [7, 9, 17, 23, 27]	$2.0 \cdot 10^{-13}$ [17]
$Z_{1,2}$	Acceptor	E_C – (0.5 – 0.7) [6, 7, 9-19, 23, 27, 32]	$1.0 \cdot 10^{-16} - 5.0 \cdot 10^{-10}$ [6, 7, 9-13, 15-18, 23, 27]	$7.0 \cdot 10^{-15} - 1.0 \cdot 10^{-13}$ [13, 15, 17]
$EH_{6,7}$	TBD Don.: [7, 15, 20, 29] Acc.: Rest	E_C – (1.35 – 1.66) [6-8, 10, 11, 13-19, 21, 27, 32]	$2.0 \cdot 10^{-18} - 9.0 \cdot 10^{-12}$ [6-8, 10, 11, 14-18, 21, 27]	$1.0 \cdot 10^{-17} - 1.0 \cdot 10^{-14}$ [14, 15, 17]
EH_4	Acceptor	E_C – (0.89 – 1.15) [6, 7, 10, 11, 16, 19-23]	$4.0 \cdot 10^{-18} - 7.0 \cdot 10^{-11}$ [6, 7, 10, 11, 16, 20, 21, 23]	–
B-center	Donor	E_V + (0.25 – 0.35) [10, 13, 23, 24, 26, 27, 32]	–	$1.0 \cdot 10^{-18} - 9.0 \cdot 10^{-11}$ [10, 13, 23, 27]
D-center	Donor	E_V + (0.37 – 0.65) [13, 23, 24-27, 32]	$3.0 \cdot 10^{-19} - 8.0 \cdot 10^{-18}$ [25]	$5.0 \cdot 10^{-18} - 9.0 \cdot 10^{-12}$ [23, 25, 27]

Range of literature values for initially considered defects

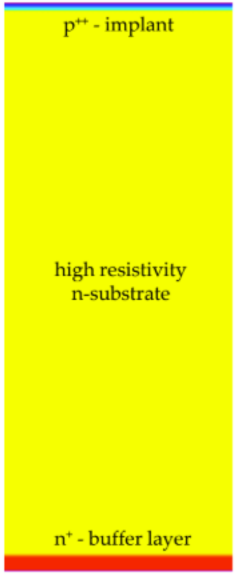

Schematics of the quasi-1D simulation structure

Philipp Gaggl HiBPM Project Review Meeting HEPHY/OEAW 4

HEPHY INSTITUTE OF HIGH ENERGY PHYSICS

ÖAW AUSTRIAN ACADEMY OF SCIENCES

- 4H-SiC challenging
  - low charge carrier concentration
  - poor parameter values
- radiation damage modeled as traps
  - energy levels in the bandgap

Material courtesy of T. Bergauer and Philipp Gaggl

Simulation results

- Charge collection efficiency (CCE) under α-irradiation [3]
- Experimental noise used as signal cut-off for simulated signals

- Very good agreement, especially for lower fluences
- Slow increase at low bias due to uniformly deposited energy in simulations

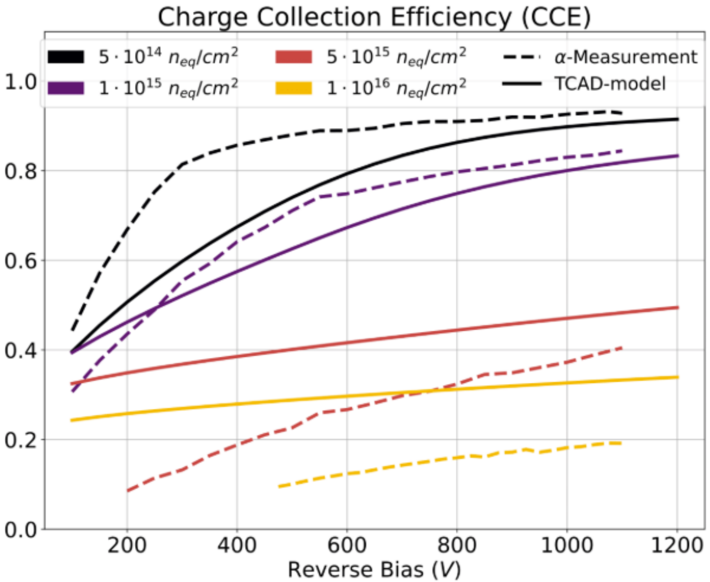

Charge collection measurement (α-particles) data from A. Gsponer [3]

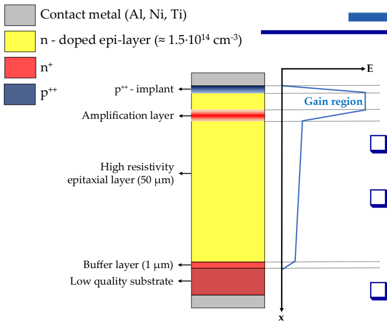

LGADs with SiC

- Design optimization.
- Additional amplification (gain) layer
- Benchmark simulations:
  - Constant epi-doping of 1.5e14 cm^{-3}
  - Gain layer doping variation

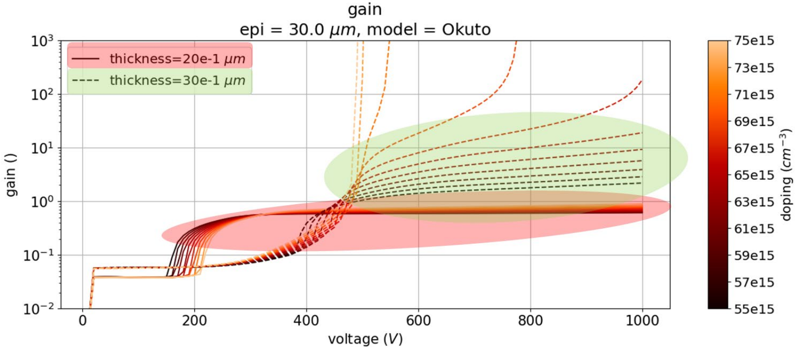

Material courtesy of T. Bergauer and Philipp Gaggl

arianna.morozzi@pg.infn.it

Rad-hard/Innovative materials

Diamond

SiC

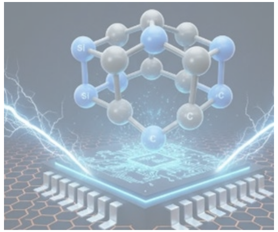

a:Si-H

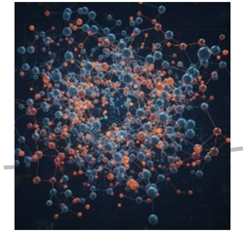

Ferroelectrics
NC-FETs

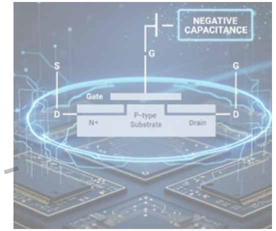

arianna.morozzi@pg.infn.it

Hydrogenated amorphous silicon (a-Si:H)

- Proposed as a suitable material to design thin a-Si:H detectors on flexible substrates (mostly Polyimide) for beam monitoring, neutron detection, and space applications.
  - intrinsic radiation tolerance, low cost, large area (different substrates, including flexible).
- Not included within the standard Synopsys TCAD material library
  - Development of a-Si:H parametric material model.
  - Different custom mobility models have been devised and implemented within the code as external PMI (Physical Model Interfaces) and accounting for different dependencies on temperature and internal potential distribution, thus resulting in a new mobility model embedded within the code.
  - Simple test structures, featuring p-i-n diodes have been simulated and compared to experimental data as a benchmark.

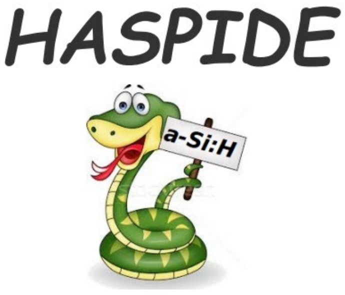

HASPIDE
and **3D-SiAm**
INFN projects

Modeling a-Si:H devices within the TCAD environment

- Not included within the standard material library
- Parameter file developed with all the characteristics
- Traps and validation of the model

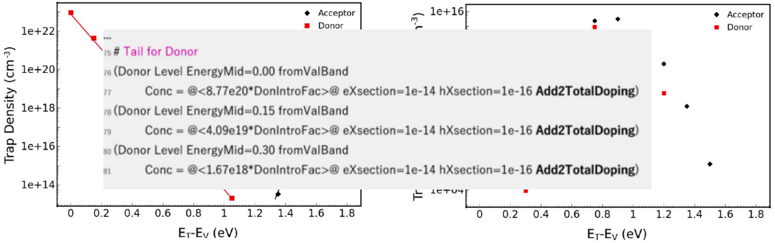

- Development of a user-defined PMI for the mobility

$$\mu = A^* V^m T^n exp\left(b\frac{\sqrt{|F|}}{T}\right)$$

HASPIDE

[D. Passeri et al., Materials Science in Semiconductor Processing, 2024, 169, 107870]

p-i-n device on kapton

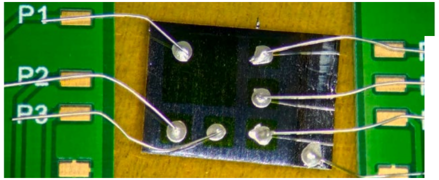

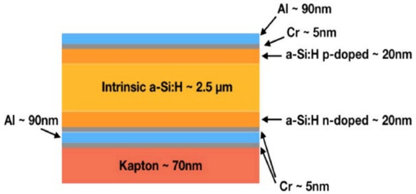

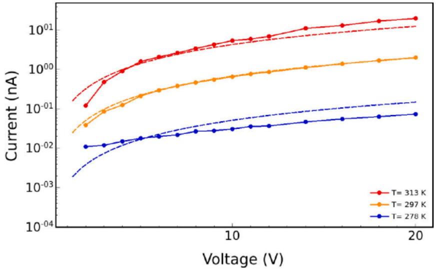

p-i-n device on crystalline Si

D. Passeri et al.

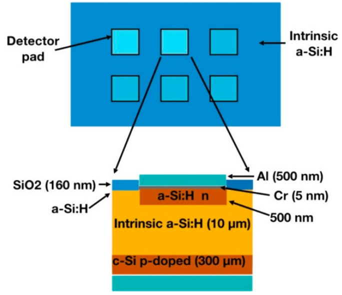

Fig. 10. p-i-n devices on crystalline silicon: simulated cross section.

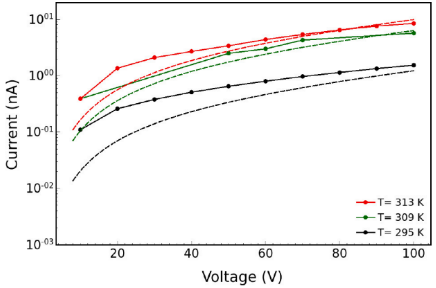

arianna.morozzi@pg.infn.it

Rad-hard/Innovative materials

Diamond

SiC

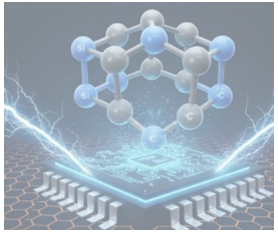

a:Si-H

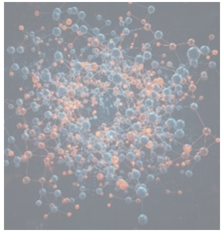

Ferroelectrics
NC-FETs

arianna.morozzi@pg.infn.it

Development of High Energy Efficient Electronic Devices Based on Innovative Ferroelectric Materials (HiEnD)

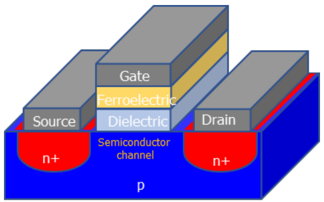

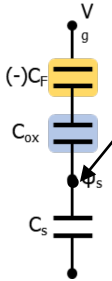

$\Psi_s > V_G$ if $C_F < 0$

Body factor Transport factor

$$SS = \frac{\partial V_g}{\partial(logI_d)} = \frac{\partial V_g}{\partial \psi_s} \times \frac{\partial \psi_s}{\partial(logI_d)}$$

$$min\left(\frac{\partial \psi_s}{\partial(logI_d)}\right) = \ln(10) \times \frac{k_B T}{q} \approx 60\ \frac{mV}{decade}$$

$$\frac{\partial V_g}{\partial \psi_s} = 1 - \frac{C_s}{C_{ins}}(\alpha_f C_{ins} - 1) \quad <1$$

Sub-threshold Swing (SS)

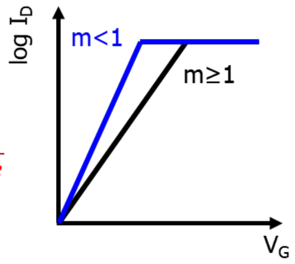

SS < 60 mV/decade typical of NC-FET

- ✓ The NegHEP project aims to investigate the radiation damage effects on Negative Capacitance Field Effect transistor
  - ✓ Issues in low signal detection in thin layers:
    - ✓ minimum detectable signal is dominated by the switching threshold of a digital switch (e.g. ≈1 ke- for 28 nm technology, <100 e- for sub 10-nm technology).
    - ✓ Continuous increase in electronics performance demand
- ✓ Proposed solution: Negative capacitance (NC) FETs
  - ✓ By replacing the standard insulator with a ferroelectric insulator of the right thickness it should be possible to implement a step-up voltage transformer that will amplify the gate voltage thus enabling low voltage/low power operation.
- ✓ Would it be possible the concept of pixelated detector with sufficiently small cells to be read out entirely by simple inverters exploiting the NC "self-amplification"?

Ferroelectric models: validation against measures

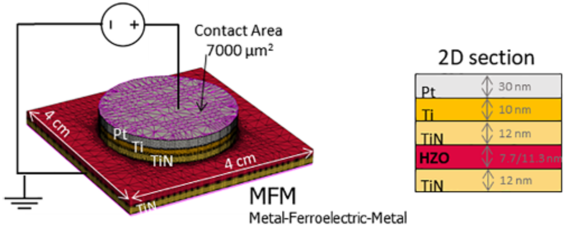

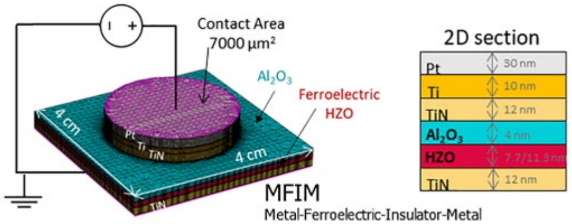

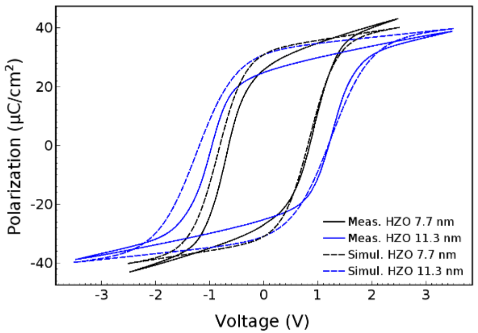

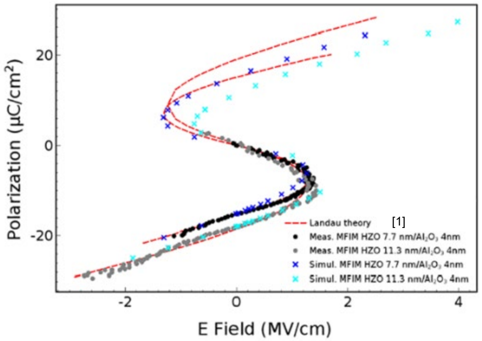

Preisach TCAD Model of hysteresis:

- ✓ remnant polarization
  Pr = 31 μC/cm²
- ✓ saturation polarization
  Ps = 33 μC/cm²
- ✓ coercive field
  Ec =1.1 MV/cm

for both 7.7 nm and 11.3 nm thin HZO films.

- Structures:
  - MFM (Metal-Ferroelectric-Metal)
    - tFE= 7.7 nm and 11.3 nm
  - MFIM (Metal-Ferroelectric-Insulator-Metal)
    - tFE= 7.7 nm and 11.3 nm
    - tDE = 0-4 nm
- Fabricated on Si substrates with ferroelectric $Hf_{0.5}Zr_{0.5}O_2$ (HZO) and dielectric Al_2O_3 thin films.
- The experimental setup has been implemented within the TCAD environment.
- Hysteretic P-E trend was realistically accounted for by using the TCAD Preisach model of hysteresis.
- The Landau S-shaped plot was realistically accounted for by using GLK hysteresis-free model.

A. Morozzi et al., Solid-State Electronics Volume 194, August 2022, 108341.
A. Morozzi et al 2022 JINST 17 C01048.
A. Morozzi et al., 2021 EuroSOI-ULIS), Caen, France, 2021, pp. 1-4, doi: 10.1109/EuroSOI-ULIS53016.2021.9560683.

Ferroelectric models: application NCFETs

- Guidelines for the optimization of the NC-FETs design.
- Capacitance matching $|C_{FE}| < C_{DE}$ for the reduction of the Sub-threshold slope.

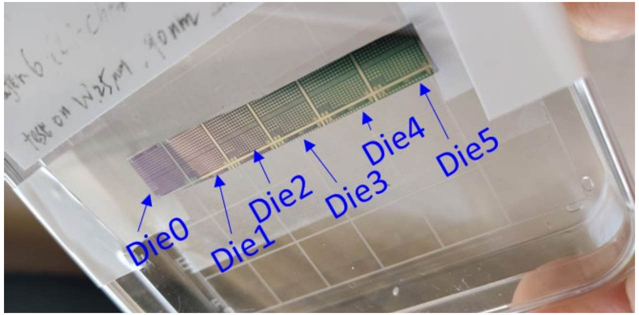

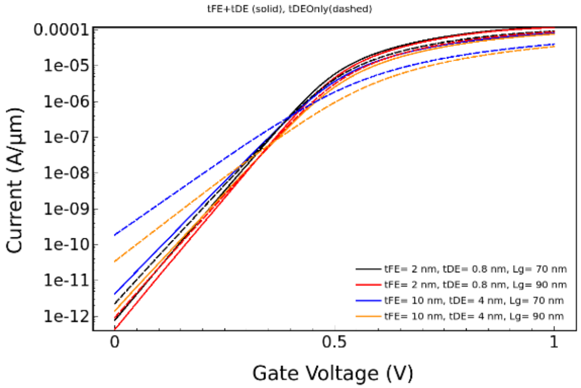

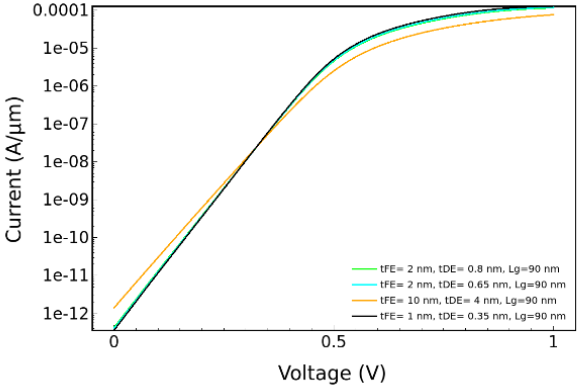

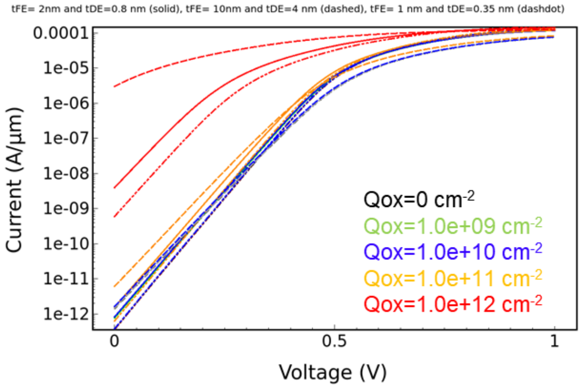

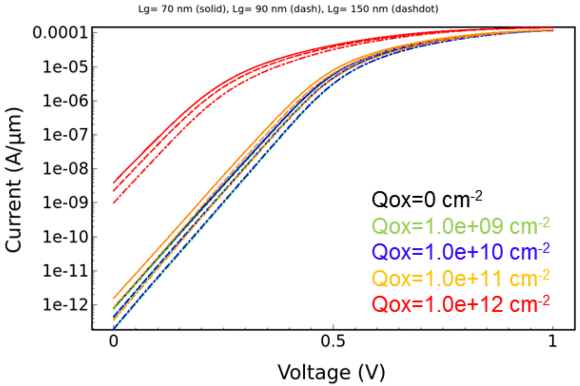

Combining TCAD and Allpix Squared

- Allpix² is a versatile, open-source simulation framework for silicon pixel detectors.
- TCAD is crucial for understanding the fabrication process and electrical characteristics of semiconductor devices, Allpix Squared complements this by providing insights into how these devices respond to particle interactions (detailed energy deposition) and the response of pixel detectors..
- The combination of these tools enables a more holistic approach to semiconductor device design, optimization, and analysis.
- Detailed E Field maps are imported from TCAD simulations to drastically improve the precision of a sensor simulation.

Sentaurus TCAD — SYNOPSYS Silicon to Software — Technology Computer-Aided Design

+

Allpix²: Monte Carlo Simulations for Semiconductor Detectors

https://doi.org/10.1016/j.nima.2018.06.020

- ★ Model semiconductor devices by means of finite element analysis
- ★ Electric Fields: accurate and realistic

- ★ Simulate full response of semiconductor detector
- ★ Particle Events: fast and high statistics

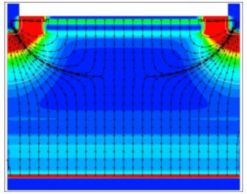

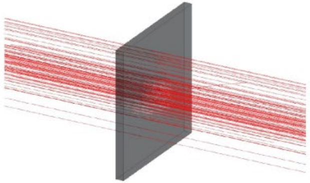

Simulation flow

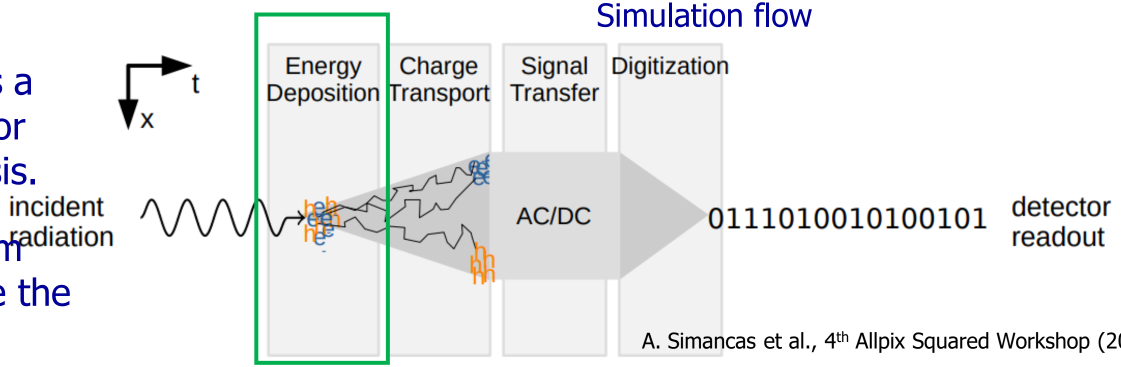

A. Simancas et al., 4th Allpix Squared Workshop (2023)

Conclusion

- ✓ Synopsys Sentaurus TCAD powerful tool to accelerate innovation and drive the industry forward.
- ✓ Sentaurus TCAD's versatility makes it suitable for a wide range of applications.
- ✓ TCAD plays a pivotal role in the design/optimization of rad-hard devices
  - Modelling radiation damage effects is a tough task!
  - New guidelines for future production of radiation-resistant options.
  - Modeling dopant removals, impact ionization, carriers’ mobility, trap dynamics
  - Every device needs specific defect modeling (LGADs for example, prone to acceptor removal)

Thank You!

BACKUP

RSD2 NPLUS W3 — Neutron Proton

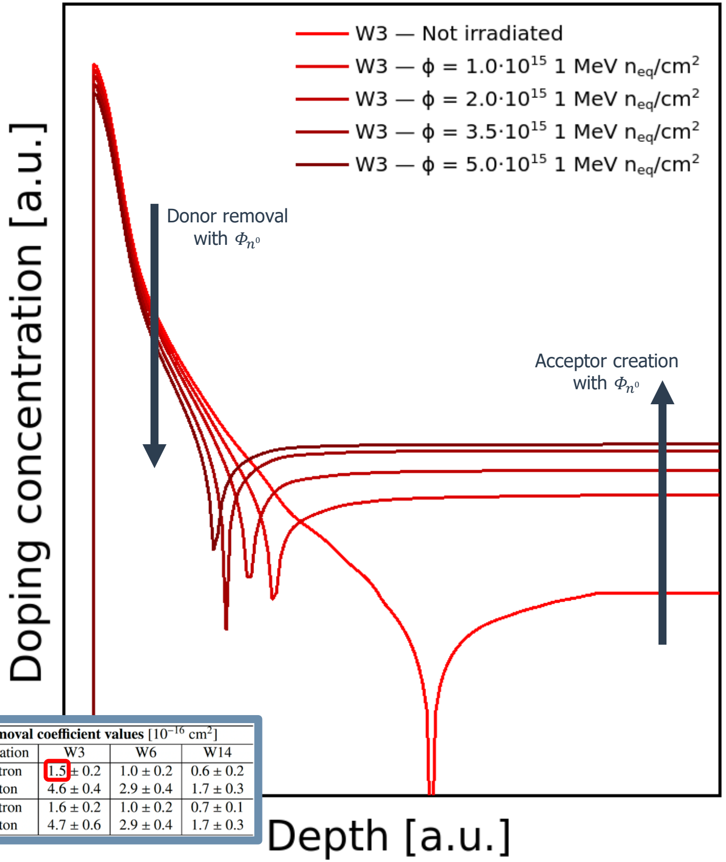

c_D donor removal coefficient values [10^{-16} cm^2]				
Location	Irradiation	W3	W6	W14
KIT	Neutron	1.5 ± 0.2	1.0 ± 0.2	0.6 ± 0.2
	Proton	4.6 ± 0.4	2.9 ± 0.4	1.7 ± 0.3
Perugia	Neutron	1.6 ± 0.2	1.0 ± 0.2	0.7 ± 0.1
	Proton	4.7 ± 0.6	2.9 ± 0.4	1.7 ± 0.3

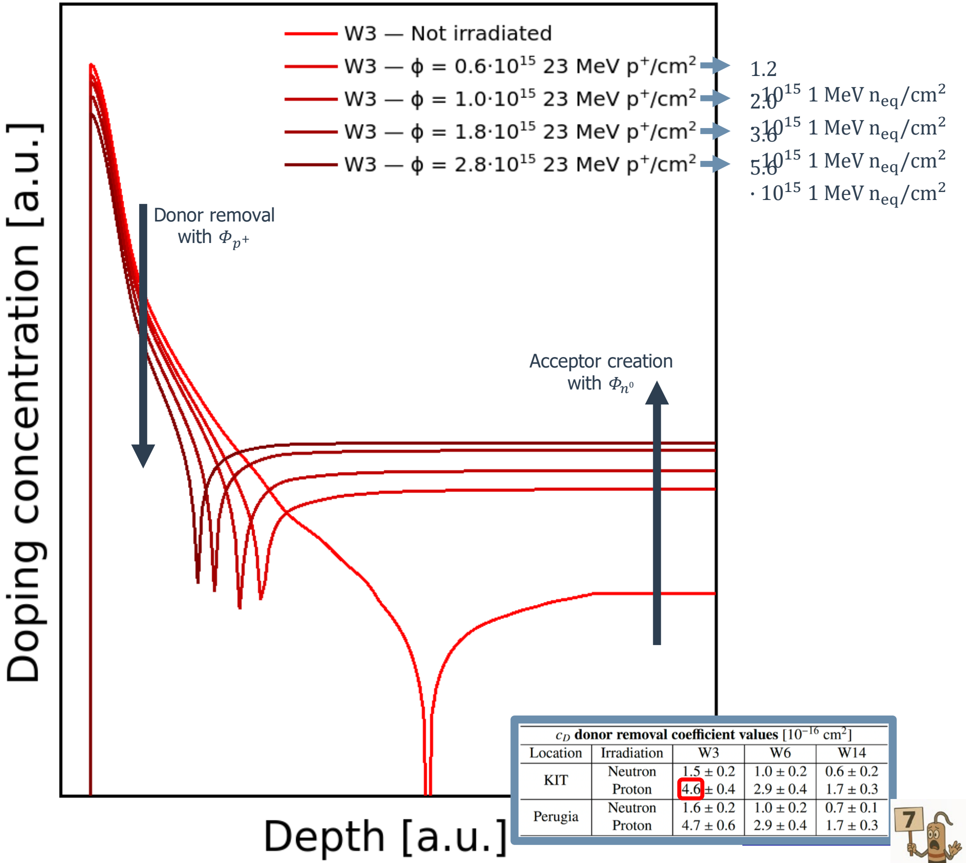

c_D donor removal coefficient values [10^{-16} cm^2]				
Location	Irradiation	W3	W6	W14
KIT	Neutron	1.5 ± 0.2	1.0 ± 0.2	0.6 ± 0.2
	Proton	4.6 ± 0.4	2.9 ± 0.4	1.7 ± 0.3
Perugia	Neutron	1.6 ± 0.2	1.0 ± 0.2	0.7 ± 0.1
	Proton	4.7 ± 0.6	2.9 ± 0.4	1.7 ± 0.3

TCAD simulation of LGAD devices

✓ **Physical models**

- **Generation/Recombination rate**
  - Shockley-Read-Hall, Band-To-Band Tunneling, Auger
  - **Avalanche Generation => impact ionization models,** *van Overstraeten-de Man, Okuto-Crowell, Massey*[1], *UniBo*
- **Fermi-Dirac statistics**
- **Carriers mobility variation** doping and field-dependent
- **Physical parameters**
  - e-/h+ recombination lifetime

✓ **Radiation damage models: "PerugiaModDoping"**

- **"New University of Perugia model"**
  - **Combined surface and bulk** TCAD damage modeling scheme[2]
  - Traps generation mechanism
- **Acceptor removal mechanism** => $N_{GL}(\phi) = N_A(0)e^{-c\phi}$
  - where
    - **Gain Layer** (**GL**), **c** removal rate (**Torino parameterization**[3])
- **Acceptor creation**

$$N_{A,bulk} = \begin{cases} N_{A,bulk}(0) + g_c\phi, & 0 < \phi < 3E15\, n_{eq}/cm^2 \\ 4.17E13 \cdot \ln(\phi) - 1.41E15, & \phi > 3E15\, n_{eq}/cm^2 \end{cases}$$

where g_c = 0.0237 cm^{-1} (**Torino acceptor creation**)

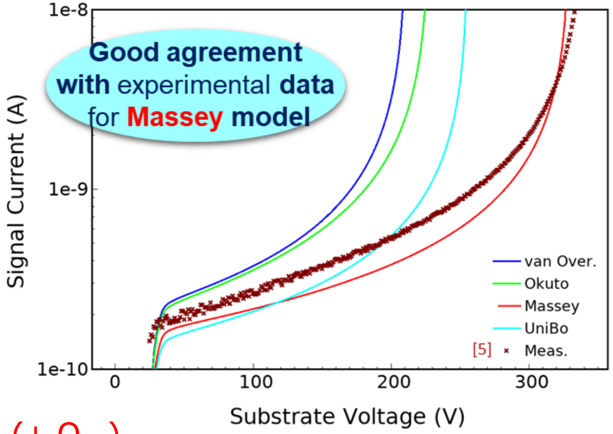

Surface damage (+ Q_{OX})

Type	Energy (eV)	Band width (eV)	Conc. (cm^{-2})
Acceptor	$E_C \le E_T \le E_C$-0.56	0.56	$D_{IT} = D_{IT}(\Phi)$
Donor	$E_V \le E_T \le E_V$+0.6	0.60	$D_{IT} = D_{IT}(\Phi)$

Bulk damage

Type	Energy (eV)	η (cm^{-1})	σ_n (cm^2)	σ_h (cm^2)
Donor	E_C - 0.23	0.006	2.3×10^{-14}	2.3×10^{-15}
Acceptor	E_C - 0.42	1.6	1×10^{-15}	1×10^{-14}
Acceptor	E_C - 0.46	0.9	7×10^{-14}	7×10^{-13}

[1] M. Mandurrino et al., IEEE NSSMIC 2017.
[2] D. Passeri, AIDA2020 report, CERN Document Server.
[3] M. Ferrero et al., https://doi.org/ 10.1016/j.nima.2018.11.121.
[4] V. Sola et al., https://doi.org/10.1016/j.nima.2018.07.060.

RSD2 batch — NF ements

c_D **donor removal coefficient values** $[10^{-16}\ cm^2]$				
Location	Irradiation	W3	W6	W14
KIT	Neutron	1.5 ± 0.2	1.0 ± 0.2	0.6 ± 0.2
	Proton	4.6 ± 0.4	2.9 ± 0.4	1.7 ± 0.3
Perugia	Neutron	1.6 ± 0.2	1.0 ± 0.2	0.7 ± 0.1
	Proton	4.7 ± 0.6	2.9 ± 0.4	1.7 ± 0.3

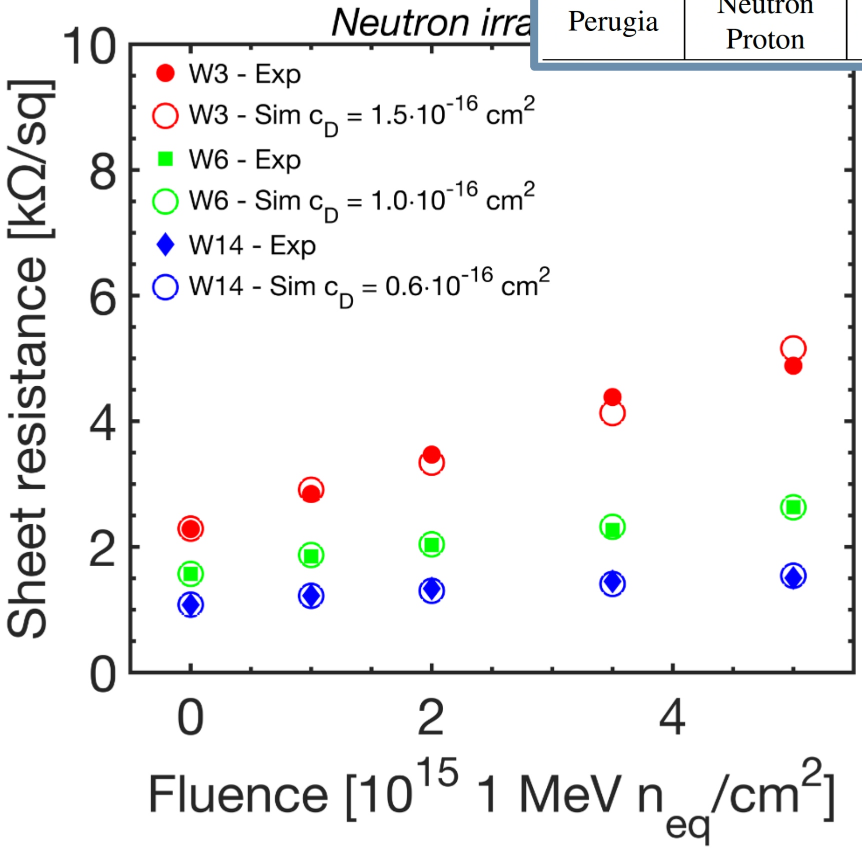

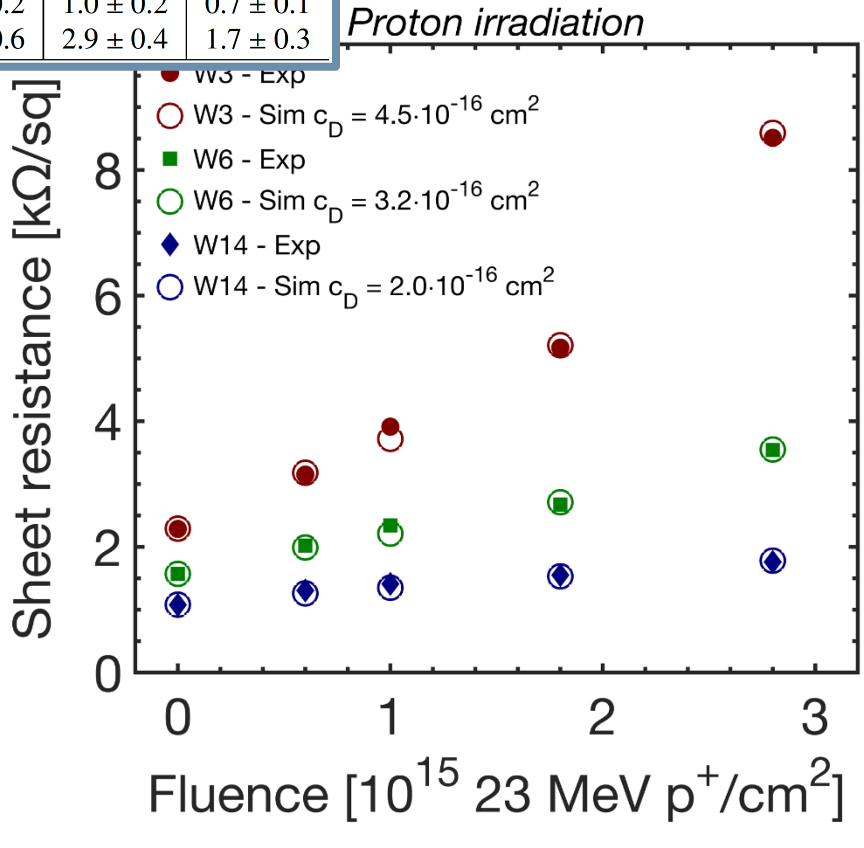

arianna.morozzi@pg.infn.it